

FACULDADE DE ENGENHARIA DA UNIVERSIDADE DO PORTO



FEUP

Multi-agent coordination with event-based communication

Pedro Vaz Teixeira

Mestrado Integrado em Engenharia Electrotécnica e de Computadores

Supervisor: Karl Henrik Johansson (Prof.)

Co-supervisor: Dimos Dimarogonas (Dr.)

Co-supervisor: João Tasso Sousa (Prof.)

August 2009

© This work is licensed under the Creative Commons Attribution-Noncommercial-Share Alike 3.0 Unported License. To view a copy of this license, visit <http://creativecommons.org/licenses/by-nc-sa/3.0/> or send a letter to Creative Commons, 171 Second Street, Suite 300, San Francisco, California, 94105, USA.

Abstract

In recent years there has been an increasing interest in mobile multi-agent systems, with the problem of how to drive a formation of N agents from one configuration to another being a key issue in many applications, particularly when each agent has limited (communication and sensing) capabilities. One such example is the navigation of glider formations, where N AUVs have to reach a target position within a given time, with sensing and communication being limited to discrete time instants. With this example as motivation, we begin by studying the single agent version of the problem, where reachability concepts are used to deal with the issue of position uncertainty, allowing us to develop two different control strategies. These strategies are then used to tackle the two-agent problem, which we generalize to obtain a partially decentralized approach to the multi-agent problem. Sufficient conditions for the successful application of these strategies, as well as the corresponding bounds on the uncertainty are also derived. The problem of estimating the disturbance set is then studied, with the objective of providing the network with increased robustness to scenarios in which there is few information about the disturbance set. Finally, using normally distributed disturbances, some relevant scenarios of both the single and multi-agent problems are simulated, which confirm the results.

Resumo

Recentemente tem havido um interesse crescente em sistemas multi-agentes móveis, sendo o problema de como conduzir uma formação de N agentes de um ponto para outro um aspecto chave em muitas aplicações, particularmente nos casos em que os agentes têm capacidades sensoriais e de comunicação limitadas. Um exemplo é a navegação de formações de *gliders*, em que N AUVs têm de atingir uma dada posição dentro de um determinado tempo, sendo a comunicação e medição restritas a certos instantes. Com este exemplo como motivação, começamos por estudar a versão do problema com um único agente, usando conceitos de atingibilidade para lidar com o problema da incerteza na posição, permitindo-nos desenvolver duas estratégias de controlo diferentes. Estas estratégias são então usadas para abordar o caso de dois agentes, que é depois generalizado para obter uma abordagem parcialmente descentralizada para o problema multi-agente. São derivadas condições suficientes à aplicação destas estratégias, assim como os correspondentes limites à incerteza. É então estudado o problema de estimar o conjunto de perturbações, com objectivo de tornar a rede mais robusta a cenários em que há pouca informação sobre as perturbações. Finalmente, usando perturbações que seguem uma distribuição normal, são simulados alguns cenários relevantes para os problemas de um e múltiplos agentes, que vêm confirmar os resultados.

Contents

Abstract	i
Resumo	iii
1 Introduction	1
1.1 Literature Review	2
1.2 Problem statement	2
1.3 Background	2
1.4 Models	4
1.4.1 Full dynamic model	5
1.4.2 Simplified model	7
2 Single agent	11
2.1 Solution to the system equation	11
2.2 Reaching the target with no disturbances	12
2.3 Reaching the target under disturbances	13
2.3.1 The disturbance set	13
2.3.2 The uncertainty set	14
2.3.3 Maximum position uncertainty	16
2.3.4 Traveling to the target	16
2.3.5 The $h_1(\cdot)$ control strategy	20
2.3.6 The $h_2(\cdot)$ control strategy	24
2.3.7 Comparative analysis of $h_1(\cdot)$ and $h_2(\cdot)$	27

2.3.8	The final approach	28
2.4	Clock drift	29
3	Multiple agents	31
3.1	Background	31
3.1.1	Graph Theory	31
3.1.2	Connectivity	32
3.2	A two-agent network	33
3.2.1	Waypoint definition	33
3.2.2	Reaching the target	34
3.2.3	Inter-agent distance	36
3.3	The multi-agent network	37
3.3.1	Waypoint definition	37
3.3.2	Connection to the two-agent network	38
3.3.3	Bounds and conditions	39
4	Disturbance set estimation	43
4.1	Background	43
4.1.1	Ellipsoids	43
4.1.2	The Normal Distribution	44
4.2	Application to the single agent problem	45
4.2.1	The average disturbance	45
4.2.2	Implications of a normally distributed disturbance set	46
4.2.3	Confidence levels	46
4.2.4	Disturbance and uncertainty sets	47
4.3	Application to the multi agent problem	49
5	Numerical Examples	51
5.1	Single agent	51
5.1.1	Trajectory	53

5.1.2	Disturbance Set Estimation	53
5.2	Multi agent	54
5.2.1	Trajectory	57
5.2.2	Connectivity	57
5.2.3	Disturbance Set Estimation	57
6	Conclusions and Future Work	75
A	Appendix	77
A.1	Disturbance Set Estimation	77
	Bibliography	82

✓

List of Figures

1.1	The graph of a piece-wise continuous function	3
1.2	Autonomous Underwater Vehicle	5
2.1	A disturbance set Ω and the corresponding over-approximating set Ω_{over}	14
2.2	Disturbance and uncertainty sets - Ω and Δ respectively. Note that $\Delta \equiv \Omega(t_{target} - t_0)$	15
2.3	Disturbance and uncertainty sets for system 2.1, given a control u that would take the system to $x(t_1)$, were there no disturbances.	15
2.4	Traveling towards the target under disturbances: estimated and true trajectories in blue and red, respectively. The true and over-approximating disturbance (Ω, Ω_{over}) and uncertainty (Δ, Δ_{over}) sets are also represented.	17
2.5	Traveling towards the target under disturbances: estimated and true trajectories in blue and red, respectively. The black circles are the uncertainty sets for each waypoint (compare with figure 2.4).	19
2.6	The effects of clock drift in the ideal stopping position and the uncertainty set. The superscript "+" denotes a time lag ($\tau > 0$) and the superscript "-" to a time lead ($\tau < 0$).	30
3.1	Network connectivity for different communication ranges.	33
3.2	A two agent network	33
3.3	Difference between the proposed waypoint assignment/transmission mechanisms	39
4.1	The ellipsoid $\mathcal{E}(c, Q)$. λ_1 denotes Q 's largest eigenvalue.	44
4.2	The confidence ellipsoids $\mathcal{E}(\mu, k^2\Sigma)$ for $k = \{1, 2, 3\}$	45
5.1	The disturbance set's confidence ellipsoids $\mathcal{E}(\mu, k^2\Sigma)$ for $k = \{1, 2, 3\}$ and the over-approximating disturbance set for examples 1 (left) and 2 (right).	59
5.2	Example 1	60

5.3	Example 2	61
5.4	Disturbance set estimation in Examples 1 (left) and 2 (right)	62
5.5	Example of a formation	63
5.6	(Example 3) Formation trajectory using the $h_1(\cdot)$ control strategy	64
5.7	(Example 3) Control signal norms for the agents in the network using the $h_1(\cdot)$ control strategy	65
5.8	(Example 3) Formation trajectory using the $h_2(\cdot)$ control strategy	66
5.9	(Example 3) Control signal norms for the agents in the network using the $h_2(\cdot)$ control strategy	67
5.10	(Example 3) Formation trajectory using the $h_1(\cdot)$ control strategy	68
5.11	(Example 4) Control signal norms for the agents in the network using the $h_1(\cdot)$ control strategy	69
5.12	(Example 4) Formation trajectory using the $h_2(\cdot)$ control strategy	70
5.13	(Example 4) Control signal norms for the agents in the network using the $h_2(\cdot)$ control strategy	71
5.14	Disturbance set estimation in Examples 3 (left) and 4 (right)	72
5.15	(Example 5) Formation trajectory using the $h_1(\cdot)$ control strategy	73
5.16	(Example 4) Formation trajectory using the $h_2(\cdot)$ control strategy	74

Chapter 1

Introduction

The deployment of a formation of several vehicles has, in some applications, several advantages over the use of just one vehicle. A far from complete account of formation control designs includes [7],[15],[14],[11],[23],[17], to name a few. In the particular case of maritime applications, an autonomous underwater vehicle (AUV) formation will take less time to cover a wider area. Also, if the sampled property has a low spatial rate of change, then the larger number of samples will result in increased data redundancy. These advantages come at a cost, namely, the complexity that arises from the coordination of the agents involved.

In multi-agent problems a common issue is that of limited communication range, which is taken into account, usually as a restriction on the inter-agent distance. However, in underwater applications there are some additional limitations. Underwater communication, for one, is typically severely constrained both in range and in bandwidth (1200 bps is a typical figure). Moreover, acoustic modems are typically power hungry and expensive. Underwater positioning is also quite challenging (GPS does not work underwater). Good navigation instruments are very expensive. This is why in some applications low cost vehicles have to surface periodically to get GPS fixes.

We take advantage of the fact that the agent has to surface to get a position fix to limit communication to these intervals, where it can use more efficient wireless modules to communicate with other agents. At the same time, since these are the only instants where we are able to have position feedback, the computation of control signals will also share this constraint. Motivated by the above observations, the goal of this thesis is to design a control strategy that drives a formation of AUVs from the initial to the target set of positions, subject to the given event constraints and under the effect of external disturbances such as ocean currents.

1.1 Literature Review

The problem presented here is related to some extent to that of real-time scheduling of control tasks. Earlier work in this area includes [19], where the authors present a method for choosing the optimal frequency for the task scheduling of the digital implementation of a controller, based on Liu and Layland's contributions on scheduling algorithms [16]. Examples of time-driven scheduling of control algorithms using feedback techniques can be found in [4, 3, 5]. In more recent years, however, and also due to the increase in interest in hybrid systems, there has been a shift towards event-driven control (EDC). Our approach shares some aspects with what is presented in [21], particularly, that the control signal is only updated when the error norm exceeds a certain threshold. Of interest is also a comparative analysis of the time and event-driven paradigms presented in [1]. EDC has also been extended to networked control systems [22], where the event triggering scheme proposed in [21] is used. The applications of EDC to both formation control and communication-constrained problems are also of interest to our problem. In [9] the authors present both centralized and distributed approaches to an agreement problem, which is considered as a simplification of the formation control problem [10].

1.2 Problem statement

The problem at hand is, given a formation of N agents (e.g. submarines), finding a control strategy that is able to drive the formation from the set of initial positions $X_0 = \bigcup_{i=1}^N x_0^i$ to the set of target positions $X_{target} = \bigcup_{i=1}^N x_{target}^i$ while meeting the following restrictions:

- Each agent can only measure its own position;
- Position measurement, as well as communication, can only take place when the agent is stopped (at the surface).

1.3 Background

We begin by recalling some useful concepts for continuous-time systems [6].

Definition 1 (Piece-wise continuous function) *A piecewise continuous function f is defined as the set of partial functions f_i such that*

$$f(t) = f_i(t), t_i \leq t < t_{i+1} \quad (1.1)$$

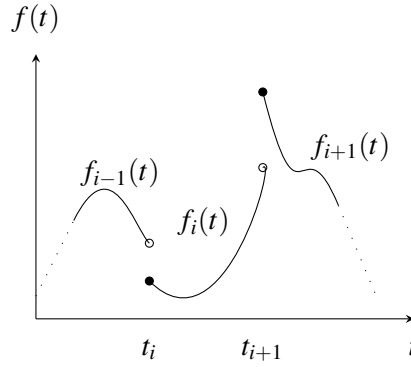


Figure 1.1: The graph of a piece-wise continuous function

Definition 2 (Admissible control signal) A control signal $u(\cdot)$ is said to be admissible if and only if

$$\forall s \in [t_0, t_1], u(s) \in \mathcal{U}(s) \quad (1.2)$$

for some (relevant) time interval $[t_0, t_1]$, where \mathcal{U} denotes the set of admissible controls.

Definition 3 (Continuous-time system) A controlled continuous-time system is described by

$$\dot{x}(t) = f(t, x(t), u(t)), u(t) \in \mathcal{U}(t) \quad (1.3)$$

where $f : \mathbb{R} \times \mathbb{R}^n \times \mathbb{R}^m \rightarrow \mathbb{R}^n$ satisfies the conditions for existence and uniqueness of ordinary differential equation. We say the system is controlled due to the presence of a controlled input, $u(t)$.

It is also important to consider the case where the system is under the influence of an external disturbance.

Definition 4 (Continuous-time system with external disturbance) A controlled continuous-time system under the effect of an external disturbance $\omega(t)$ is described by

$$\dot{x}(t) = f(t, x(t), u(t), \Omega(t)), u(t) \in \mathcal{U}(t), \omega(t) \in \Omega(t) \quad (1.4)$$

where $f : \mathbb{R} \times \mathbb{R}^n \times \mathbb{R}^m \times \mathbb{R}^p \rightarrow \mathbb{R}^n$ satisfies the conditions for existence and uniqueness of ordinary differential equation.

Similarly to what happens for the control input, the disturbance signal must also lie in a set, so definition 2 also applies to $w(s)$, with the set of admissible controls \mathcal{U} replaced by the disturbance

set, \mathcal{W} .

Another key concept in this approach to multi-agent systems is that of forward reachable set¹.

Definition 5 (Reachable set departing from a point) *Suppose a system described by (1.3) is at x_0 , at time t_0 . The reachable set $\mathcal{R}[\tau, x_0, t_0]$ of the system at time $\tau \geq t_0$ starting from x_0 at time t_0 is given by:*

$$\mathcal{R}_{\mathcal{U}}[\tau, x_0, t_0] = \bigcup_{u(s) \in U(s)} \left\{ x(\tau) : x(\tau) = \int_{t_0}^{\tau} f(s, x(s), u(s)) ds, u(s) \in U(s), s \in (t_0, \tau) \right\} \quad (1.5)$$

Finally, we generalize the reachable set concept for a system under the presence of an external disturbance.

Definition 6 (Reachable set departing from a point under external disturbance) *Suppose a system described by (1.4) is at x_0 , at time t_0 . The reachable set $\mathcal{R}_{\mathcal{U}, \Omega}[\tau, x_0, t_0]$ of the system at time $\tau \geq t_0$ starting from x_0 at time t_0 is given by:*

$$\mathcal{R}_{\mathcal{U}, \Omega}[\tau, x_0, t_0] = \bigcup_{u(s) \in U(s), \omega(s) \in \Omega(s)} \left\{ x(\tau) : x(\tau) = \int_{t_0}^{\tau} f(s, x(s), u(s), \omega(s)) ds, u(s) \in U(s), \omega(s) \in \Omega(s), s \in (t_0, \tau) \right\} \quad (1.6)$$

1.4 Models

Let the ideal dynamics of the vehicle be described by equation 1.3. We assume that, when present, disturbances are additive, that is,

$$\dot{x}(t) = f(t, x(t), u(t)) + \omega(t) \quad (1.7)$$

where $\omega(t) \in \Omega(t), \forall t \in [t_0, t_1]$. This being true, we can study the effect of the disturbances separately from the system's dynamics. As a consequence, the uncertainty set (which we will later define) becomes independent from the vehicle's dynamics. Throughout the rest of the document we will be modeling the vehicle as a two-dimensional integrator (equation 1.3) for the sake of simplicity. However, two relevant vehicle models will be presented next, summarizing some of the main results in [20, 12].

¹Throughout this document we will refer to it simply as reachable set.

1.4.1 Full dynamic model

To describe the full dynamic model of an underwater vehicle, we first have to introduce two different reference frames. The first one is the *Earth-fixed* frame, whose origin is located at an arbitrary point on the Earth's surface, with the directions of the axes given by the so-called North-East-Down convention: x points North, y points East, and z points down. The other is the *body-fixed* reference frame, where the origin is (usually) fixed at the vehicle's center of mass and the axes coinciding with the principal axes of inertia of the vehicle (figure 1.2). In order to express the

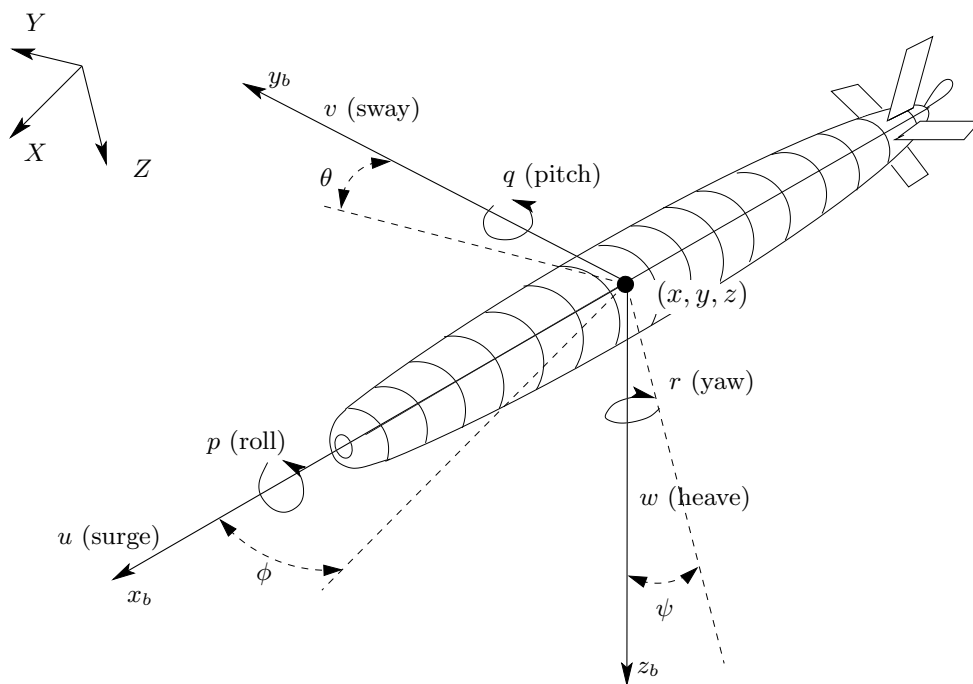


Figure 1.2: Autonomous Underwater Vehicle

vehicle state in either one of these reference frames, we will need a total of six variables - three to describe its position and another three to describe its attitude. Since we are interested in the vehicle's motion in both of these frames, we will need a total of twelve variables, as well as an equation that relates one frame to the other.

In the body-fixed reference frame, the vehicle's motion is described by six velocity components

- u - linear speed along the x_b axis (surge) [m/s],
- v - linear speed along the y_b axis (sway) [m/s],
- w - linear speed along the z_b axis (heave) [m/s],

- p - angular speed along the x_b axis (roll speed) [rad/s],
- q - angular speed along the y_b axis (pitch speed) [rad/s],
- r - angular speed along the z_b axis (yaw speed) [rad/s]

which we represent as the vector

$$\mathbf{v} = [u, v, w, p, q, r]^T \quad (1.8)$$

For the Earth-fixed reference frame, we have

- x - position w.r.t the x axis (North) [m],
- y - position w.r.t the y axis (East) [m],
- z - position w.r.t the z axis (down) [m],
- ϕ - heading (yaw) angle w.r.t the reference axes [rad],
- θ - pitch angle w.r.t the reference axes [rad],
- ψ - roll angle w.r.t the reference axes [rad]

which we represent as the vector

$$\boldsymbol{\eta} = [x, y, z, \phi, \theta, \psi]^T \quad (1.9)$$

The evolution of $\boldsymbol{\eta}$ is related to \mathbf{v} by the following kinematic equation

$$\dot{\boldsymbol{\eta}} = J(\boldsymbol{\eta})\mathbf{v} \quad (1.10)$$

where

$$J_1(\boldsymbol{\eta}) = \begin{bmatrix} \cos \theta \cos \psi & \sin \phi \sin \theta \cos \psi - \cos \phi \sin \psi & \cos \phi \sin \theta \cos \psi + \sin \phi \sin \psi \\ \cos \theta \sin \psi & \sin \phi \sin \theta \sin \psi + \cos \phi \cos \psi & \cos \phi \sin \theta \sin \psi - \sin \phi \cos \psi \\ -\sin \theta & \cos \theta \sin \psi & \cos \theta \cos \phi \end{bmatrix}$$

$$J_2(\boldsymbol{\eta}) = \frac{1}{\cos \theta} \begin{bmatrix} \cos \theta & \sin \phi \sin \theta & \cos \phi \sin \theta \\ 0 & \cos \phi \cos \theta & -\sin \phi \cos \theta \\ 0 & \sin \phi & \cos \phi \end{bmatrix}$$

$$J(\boldsymbol{\eta}) = \begin{bmatrix} J_1(\boldsymbol{\eta}) & 0 \\ 0 & J_2(\boldsymbol{\eta}) \end{bmatrix}$$

Using the principle of superposition, we can incorporate the effect of water current velocity by considering that \mathbf{v} is relative to a frame moving with the surrounding water mass with a velocity

$$\mathbf{v}_c = [v_{cx}, v_{cy}, v_{cz}, 0, 0, 0] \quad (1.11)$$

measured in the earth-fixed reference frame. Equation 1.10 becomes

$$\dot{\boldsymbol{\eta}} = \mathbf{J}(\boldsymbol{\eta})\mathbf{v} + \mathbf{v}_c \quad (1.12)$$

Finally, as for the vehicle dynamics themselves, these are described by the following equation

$$\mathbf{M}\dot{\mathbf{v}} + \mathbf{C}(\mathbf{v})\mathbf{v} + \mathbf{D}(\mathbf{v})\mathbf{v} + \mathbf{g}(\boldsymbol{\eta}) = \mathbf{F}_{act} \quad (1.13)$$

where \mathbf{M} is the constant inertia and added mass matrix, $\mathbf{C}(\mathbf{v})$ is the Coriolis and centripetal matrix, $\mathbf{D}(\mathbf{v})$ is the damping matrix, $\mathbf{g}(\boldsymbol{\eta})$ is the vector of restoring forces and moments and \mathbf{F}_{act} is the vector representing the forces from the actuators, expressed in the body-fixed reference frame.

1.4.2 Simplified model

Using the reasoning exposed in ([2, 20]), we can approximate the vehicle dynamics using the unicycle model:

$$\begin{bmatrix} \dot{x}_1(t) \\ \dot{x}_2(t) \\ \dot{x}_3(t) \end{bmatrix} = \begin{bmatrix} u_1(t) \cos(x_3(t)) \\ u_1(t) \sin(x_3(t)) \\ u_2(t) \end{bmatrix} \quad (1.14)$$

where the controls $u_1(t)$ and $u_2(t)$ denote the linear and angular speeds respectively. The control signal $[u_1(t), u_2(t)]^T$ is, of course, restricted to be in the set of admissible controls, \mathcal{U} . This set can, for example, be expressed as a set of bounds on the linear and angular speeds:

$$\mathcal{U} = \{[u_1(t), u_2(t)]^T \in \mathbb{R}^2 : \|u_1(t)\| \leq u_{1(max)} \wedge \|u_2(t)\| \leq u_{2(max)}\} \quad (1.15)$$

where $u_{1(max)}$ would be the the maximum speed relative to the surrounding water mass and $u_{2(max)}$ the maximum turning rate.

Connection to the two-dimensional integrator model

If instead of the center point $[x_C; y_C]^T$ of the vehicle, we control a point $[x; y]^T$ at a distance l from the center along the positive direction of $u_1(t)$, we can treat the vehicle dynamics as a simple integrator [13]. This way, we can use the vehicle's desired velocity in Cartesian coordinates,

which we denote by $u^C(t) = [u_1^C(t), u_2^C(t)]^T$ to determine the corresponding linear and angular speeds, $u_1(t)$ and $u_2(t)$:

$$\begin{bmatrix} u_1(t) \\ u_2(t) \end{bmatrix} = A(x_3(t))^{-1} \cdot u^C(t) \quad (1.16)$$

where the decoupling matrix A is written as

$$A(x_3(t)) = \begin{bmatrix} \cos(x_3(t)) & -l \cdot \sin(x_3(t)) \\ \sin(x_3(t)) & l \cdot \cos(x_3(t)) \end{bmatrix}$$

The vehicle dynamics are thus described by

$$\begin{aligned} \dot{x}(t) &= u^C(t) \\ \begin{bmatrix} u_1(t) \\ u_2(t) \end{bmatrix} &= A(x_3(t))^{-1} \cdot u^C(t) \\ \dot{x}_3(t) &= u_2(t) \end{aligned} \quad (1.17)$$

We now see that although we'll be using the two-dimensional integrator model, it is easy to relate this model to the unicycle. Also, notice that (1.17) is an example of a continuous-time system just as described by definition 3. As such, it is also important to characterize the set of admissible controls, \mathcal{U} . Keeping in mind the admissible set definition we provided for the unicycle model, we now have to relate it with the model above. Noticing that the norm of $u^C(t)$ is the vehicle's linear speed, $u_1(t)$, we keep this restriction. We're now left with the upper bound on the turning rate, and it is here that we make a strong assumption on $u^C(t)$, by assuming that it is such that this restriction is always satisfied. This way, for the model described by 1.17, we have that the admissible control set is defined by

$$\mathcal{U} = \{u^C(t) = [u_1^C(t), u_2^C(t)]^T \in \mathbb{R}^2 : \|u^C(t)\| \leq u_{1(max)}\} \quad (1.18)$$

Disturbances

Finally, we refine equation 1.17 so as to include the effect of external disturbances. And since we have assumed disturbances to be additive, we get

$$\begin{aligned} \dot{x}(t) &= u^C(t) + \omega(t) \\ \begin{bmatrix} u_1(t) \\ u_2(t) \end{bmatrix} &= A(x_3(t))^{-1} \cdot u^C(t) \\ \dot{x}_3(t) &= u_2(t) \end{aligned} \quad (1.19)$$

Similarly to what happened with the previous model, we now have an example of a continuous-time system that fits the description given by definition 4. Even though we keeping our charac-

terization of (U) , we do not explicitly define Ω , the set where the disturbances lie in, with the justification that this set might be unknown. Still, in the next chapter, we will make some assumptions on Ω that will facilitate dealing with this issue.

Chapter 2

Single agent

2.1 Solution to the system equation

The first step we take to solve the single agent problem is to derive the solution to the system equation,

$$\dot{x}(t) = u(t) + \omega(t) \quad (2.1)$$

We choose this simple equation for the reasons considered in the previous chapter. To obtain the agent's position at some instant t , we integrate the equation above

$$\int_{t_0}^t \dot{x}(\tau) d\tau = \int_{t_0}^t (u(\tau) + \omega(\tau)) d\tau$$

Given the initial condition $x(t_0) = x_0$, the equation becomes

$$x(t) = x_0 + \int_{t_0}^t (u(\tau) + \omega(\tau)) d\tau \quad (2.2)$$

Now, we let $u(t)$ be an admissible and piecewise continuous control signal,

$$u(t) = \bigcup_{i=0}^{N-1} u_{i,i+1}(t) \quad (2.3)$$

such that $u_{i,i+1} : [t_i, t_{i+1}] \rightarrow \mathbb{R}^2, \forall i \in \{0, 1, \dots, N-1\}$. Replacing in 2.2 yields

$$x(t) = x_0 + \sum_{i=0}^{k-1} \left(\int_{t_i}^{t_{i+1}} (u_{i,i+1}(\tau) + \omega(\tau)) d\tau \right) + \int_{t_k}^t (u_{k,k+1}(\tau) + \omega(\tau)) d\tau \quad (2.4)$$

where k is such that $t \in [t_k, t_{k+1}]$. We proceed by making a stronger assumption (for reasons which will later become clear): the control signal $u(t)$ is not only continuous in each interval $[t_i, t_{i+1}]$,

but it is also constant: $u_{i,i+1}(t) = u_{i,i+1}$. Also, we are only interested in the agent's position at the discontinuities, that is, $x(t)$ for $t = t_k$, with $k \in \{0, 1, \dots, N\}$, so we now have

$$\begin{aligned} x(t_k) &= x_0 + \sum_{i=0}^{k-1} \left(u_{i,i+1} (t_{i+1} - t_i) + \int_{t_i}^{t_{i+1}} \omega(t) dt \right) \\ &= x_0 + \sum_{i=0}^{k-1} (u_{i,i+1} (t_{i+1} - t_i) + \delta_{i+1}) \end{aligned} \quad (2.5)$$

where we have denoted the *position drift* in the interval $[t_i, t_{i+1}]$ by δ_{i+1} :

$$\delta_{i+1} = \int_{t_i}^{t_{i+1}} \omega(t) dt \quad (2.6)$$

Under the given assumptions, we call equation 2.5 the solution to the system equation.

2.2 Reaching the target with no disturbances

In the single-agent version of the problem, we want to find a control strategy that drives the agent to x_{target} at time t_{target} , starting from x_0 at time t_0 . Before devising such a control strategy, we must determine if the target can be reached in the specified time using an admissible control law. Note that it is a particular type of reachability that is relevant to our problem: *reaching a position within a given amount of time*, as opposed to *a position being reachable or not*.

Recalling definition 6, we can say that x_{target} is reachable if and only if

$$x_{target} \in \mathcal{R}_{\mathcal{U}, \Omega} [t_{target}, x_0, t_0] \quad (2.7)$$

that is, if the target position is in the set of all the positions that are reachable within the given time using an admissible control signal. Choosing, for example, the following control signal

$$u^*(t) = (x_{target} - x_0)(t_{target} - t_0)^{-1} \quad (2.8)$$

it is easy to see that, assuming there are no disturbances ($\omega(t) = 0, t \in [t_0, t_{target}]$), we will reach the target at the specified time. We now need to check whether this control signal is admissible. Recalling the definition of \mathcal{U} from the previous subsection

$$\mathcal{U} = \{u | \forall t \in [t_0, t_1], \|u(t)\| \leq u_{max}\} \quad (2.9)$$

we see that we need to compute $\|u\|$, which is simply

$$\|u\| = \frac{\|x_{target} - x_0\|}{t_{target} - t_0} \quad (2.10)$$

The reason behind the choice of this particular control signal is that it is optimal for the model that we're using. Here, the word optimal is used in the following sense: given a target $\{x_{target}, t_{target}\}$ and a starting position, $\{x_0, t_0\}$, u^* control signal that uses the least amount of energy and for which the target is reached in the given time. And, since using the least amount of energy also implies having the smallest p -norm, we can say that if the target isn't reachable setting $u = u^*$, then it isn't reachable.

We can now state this as the *reachability condition under ideal conditions*:

Condition 1 (Reachability condition under no disturbances) *Let x_0 be the vehicle position at time t_0 , and x_{target} the desired position at time t_{target} . We say this position is reachable in the specified time if and only if*

$$\frac{\|x_{target} - x_0\|}{t_{target} - t_0} \leq u_{max} \quad (2.11)$$

and it can be reached by setting the control as in equation 2.8.

2.3 Reaching the target under disturbances

We now try to solve the same problem for the scenario in which the agent is subject to external speed disturbances (recall equation 1.19). To determine whether or not the target is reachable, it is no longer enough to use condition 2.8, as it does not capture the effects of the external disturbances. We could compute the reachable set for $\dot{x}(t) = f(t, x(t), u(t), \omega(t))$, with $\omega(t) \in \Omega$, but since little might be known about Ω , this might prove hard. Instead, given a control signal $u(t)$, we set to determine the set of all different positions that the vehicle can reach, due to the presence of disturbances - the *uncertainty set*.

2.3.1 The disturbance set

Since Ω is not known and/or may be too complex to work with, we begin by constructing an over-approximation, taking into account an *upper bound on the external disturbance*:

$$\gamma \geq \max(\|\omega\|) \quad (2.12)$$

The over-approximating set is thus defined as

$$\Omega_{over} = \{\omega : \|\omega\| \leq \gamma\} \quad (2.13)$$

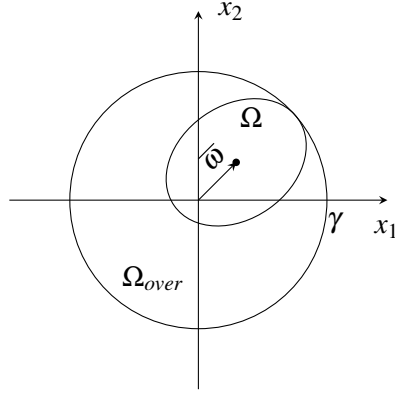


Figure 2.1: A disturbance set Ω and the corresponding over-approximating set Ω_{over}

Notice that γ is just an upper bound on the position uncertainty growth rate, that allows us to quantify (from a worst-case perspective) the uncertainty in the vehicle's position as a linear function of time.

2.3.2 The uncertainty set

We want to find the *uncertainty set* for the system $\dot{x}(t) = u(t) + \omega(t)$ at time t_{target} : $\Delta(t_{target})$. This can be seen as the equivalent of finding the reachable set for the system

$$\dot{x}(t) = \omega(t), \text{ with } x(t_0) = 0, \omega(t) \in \Omega(t), \forall t \in [t_0, t_{target}] \quad (2.14)$$

We begin by assuming that $\Omega(t)$ is constant in $[t_0, t_{target}]$ and has zero mean, which means that Ω is centered around the origin. For this particular scenario, the reachable set is fairly easy to compute:

$$\mathcal{R}[t_{target}, 0, t_0] = \bigcup_{\omega(t) \in \Omega(t)} \left\{ x(t_{target}) : x(t_{target}) = \int_{t_0}^{t_{target}} \omega(t) dt \right\} \quad (2.15)$$

$$= \Omega(t_{target} - t_0) \quad (2.16)$$

which is just the disturbance set Ω scaled by a factor of $(t_{target} - t_0)$. The scaling (relative to the origin) of a set by a scalar k is obtained by, for all points x in the original set S , multiplying x by k to obtain the corresponding element in the scaled set kS . This can be easily demonstrated by choosing a constant $\omega \in \partial\Omega$ (where ∂ denotes the boundary of a set) and computing $x(t_{target})$ for system 1.7. The reachable set is then centered around the origin as the mean disturbance is zero. If this is not true, then the center will instead be at $\bar{\omega}(t_{target} - t_0)$.

Returning to the ideal system, let $u(t)$ be an admissible control signal. Then

$$x(t_{target}) = x(t_0) + \int_{t_0}^{t_{target}} f(t, x(t), u(t)) dt$$

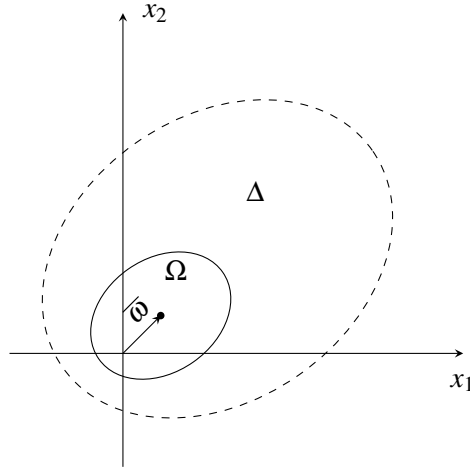


Figure 2.2: Disturbance and uncertainty sets - Ω and Δ respectively. Note that $\Delta \equiv \Omega(t_{target} - t_0)$.

will be the system's position at time t_{target} . We can now make use of these results to obtain the uncertainty set for the system with disturbances at time $t_{target} - \Delta(t_{target})$ - which will be the set $(t_{target} - t_0)\Omega$ centered at $x(t_{target}) + \bar{w}(t_{target} - t_0)$.

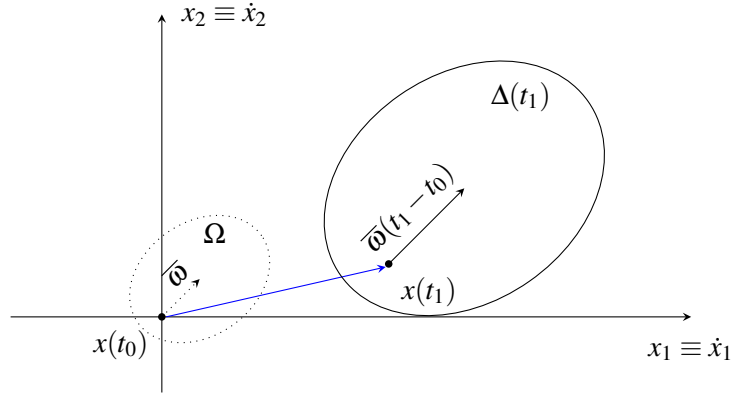


Figure 2.3: Disturbance and uncertainty sets for system 2.1, given a control u that would take the system to $x(t_1)$, were there no disturbances.

The motivation behind constructing the over-approximating set is now clear: if Ω isn't known, we instead work with Ω_{over} to obtain the corresponding over-approximated uncertainty set, $\Delta_{over}(t_{target})$. And since Ω_{over} is, by construction, centered around the origin, $\Delta_{over}(t_{target})$ is simply Ω_{over} scaled by a factor of $(t_{target} - t_0)$ centered at $x(t_{target})$. Consequently,

$$\|x(t_{target}) - x_{target}\| \leq \gamma(t_{target} - t_0) \quad (2.17)$$

or, more generically,

$$\|x(t_1) - x_{est}(t_1)\| \leq \gamma(t_1 - t_0) \quad (2.18)$$

where $x_{est}(t_1)$ is the ideal position at time t_1 .

2.3.3 Maximum position uncertainty

One of the advantages of considering the over-approximating sets is clearly shown by equation 2.18. Assuming that, for some reason, we don't want to be more than ε meters away from the ideal trajectory, we can use that equation to compute the minimum (worst-case) time the position uncertainty takes to reach ε .

$$t_\varepsilon = \frac{\varepsilon}{\gamma} \quad (2.19)$$

At the end of that time (that is, at $t = t_0 + t_\varepsilon$), the agent should stop to take a position measurement and check the distance to the ideal/planned path. Moreover, with Ω being constant, the agent should also stop every t_ε seconds. We let

$$t_{target} = t_0 + N \cdot t_\varepsilon + t_f \quad (2.20)$$

where

$$N = \left\lfloor \frac{(t_{target} - t_0)}{t_\varepsilon} \right\rfloor \quad (2.21)$$

and

$$t_f = (t_{target} - t_0) \bmod t_\varepsilon \quad (2.22)$$

that is, t_f is the remainder after integer division of $t_{target} - t_0$ by t_ε . Again, notice that with equation 2.21 we have implicitly assumed that γ is constant from t_0 to t_{target} , and consequently, the i -th stopping (surfacing) time can be expressed as

$$t_i = t_0 + i \cdot t_\varepsilon \quad (2.23)$$

The interpretation for this is that while traveling towards the target, the agent will stop N times, taking a total of $N \cdot t_\varepsilon$ seconds, before making its final approach to the target, which will take only t_f seconds.

2.3.4 Traveling to the target

The vehicle starts at $x = x_0$ at time $t = t_0$. Using a control strategy $u(t) = h(\cdot)$ that is assumed to be able to take the agent to the target in the specified time, it computes $u(t) = u_{0,1}(t)$, which will

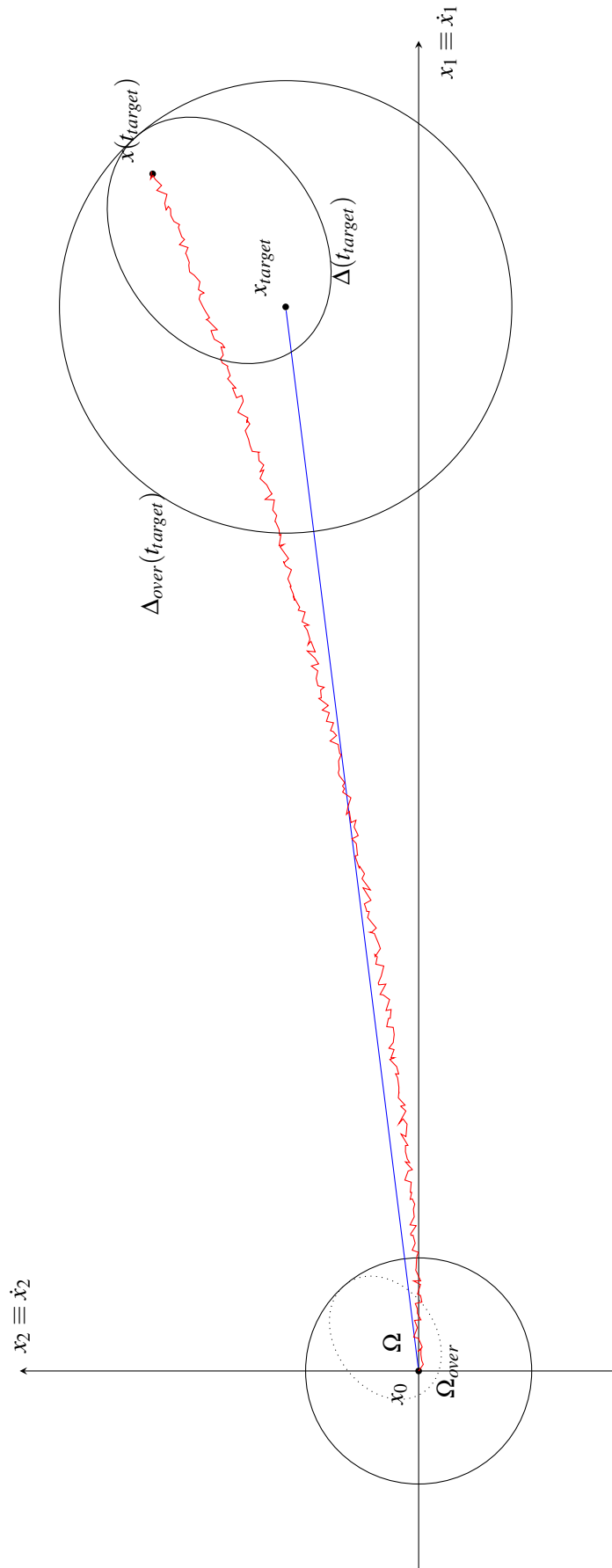


Figure 2.4: Traveling towards the target under disturbances: estimated and true trajectories in blue and red, respectively. The true and over-approximating disturbance (Ω, Ω_{over}) and uncertainty (Δ, Δ_{over}) sets are also represented.

drive it to the first stopping point, X_1 . Under no disturbances, the first stopping point would be located at

$$W_1 = x_0 + \int_{t_0}^{t_1} u_{0,1}(t) dt$$

where $t_1 = t_0 + t_\varepsilon$. We call this particular stopping point (i.e., where the agent would stop under ideal conditions) a *waypoint*. In reality, since the system is under the influence of an external disturbance $\omega(t)$, the stopping position will most likely be different from the waypoint:

$$\begin{aligned} x_1 &= x_0 + \int_{t_0}^{t_1} u_{0,1}(t) dt + \int_{t_0}^{t_1} \omega(t) dt \\ &= W_1 + \delta_1 \end{aligned}$$

where we have denoted the position drift from x_0 to x_1 by δ_1 (recall equation 2.6).

Generically, waypoint $i + 1$ will be located at

$$W_{i+1} = x_i + \int_{t_i}^{t_{i+1}} u_{i,i+1}(t) dt \quad (2.24)$$

and the corresponding stopping position will be

$$x_{i+1} = W_{i+1} + \delta_{i+1} \quad (2.25)$$

Notice that because of the way we have defined γ , we can guarantee that

$$\|\delta_i\| \leq \varepsilon, \forall i \in \{1, 2, \dots, N\} \quad (2.26)$$

Denoting our control strategy as $h(\cdot)$, we summarize this approach with algorithm 1.

Algorithm 1 Main approach

Require: $\gamma \geq \|\omega\|$

1: $t_\varepsilon \leftarrow \varepsilon \gamma^{-1}$

2: $N \leftarrow \left\lfloor \frac{(t_{\text{target}} - t_0)}{t_\varepsilon} \right\rfloor$

3: **for** $i = 0$ to $N - 1$ **do**

4: $t_{i+1} = t_i + t_\varepsilon$

5: $u_{i,i+1} = h(\cdot)$

6: $W_{i+1} = x_i + \int_{t_i}^{t_{i+1}} u_{i,i+1}(t) dt$

7: $\delta_{i+1} = \int_{t_i}^{t_{i+1}} \omega(t) dt$

8: $x_{i+1} = W_{i+1} + \delta_{i+1}$

9: **end for**

Having summarized how to reach the target, we now need to devise at least one control strategy $h(\cdot)$ that ensures we reach it.

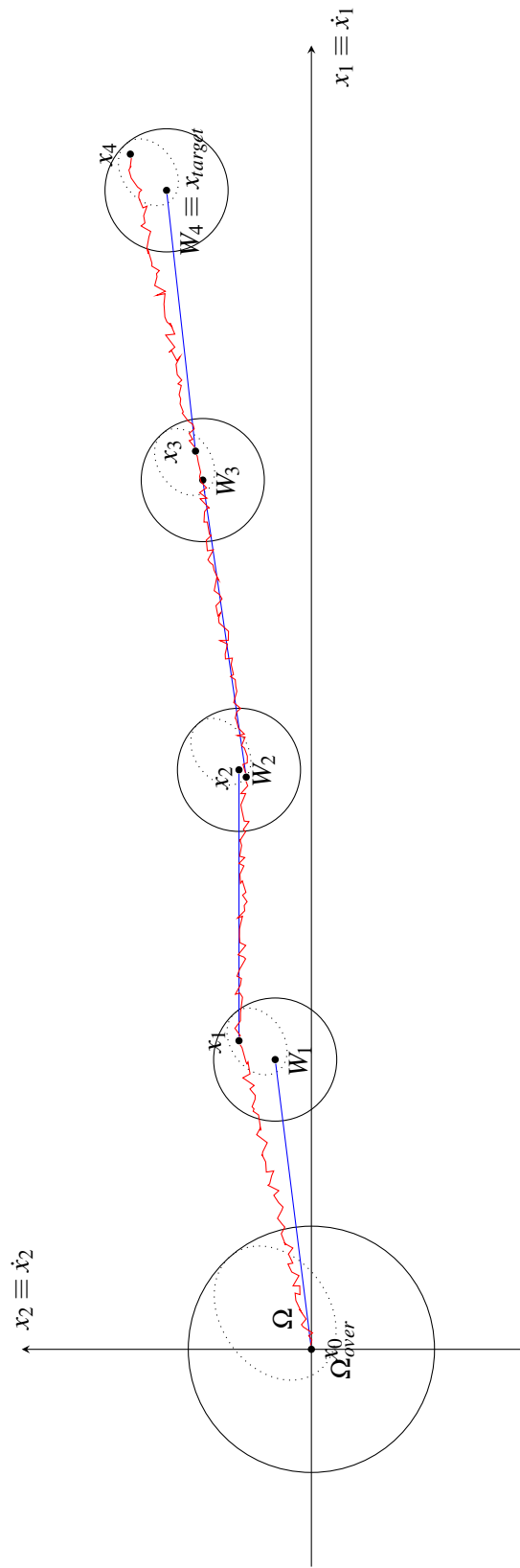


Figure 2.5: Traveling towards the target under disturbances: estimated and true trajectories in blue and red, respectively. The black circles are the uncertainty sets for each waypoint (compare with figure 2.4).

2.3.5 The $h_1(\cdot)$ control strategy

When dealing with the problem of reaching the target under no disturbances, we saw that the control signal defined by equation 2.8 was, under those conditions, optimal. We could then start with $u(t)$ defined in such a way and, at each stopping position, update $u(t)$ using the same control strategy, but with the current position and time. We call this control strategy $h_1(\cdot)$, and the main results for it follow:

Theorem 1 (Target reachability using control strategy $h_1(\cdot)$) *Let*

$$\begin{aligned} u_{i,i+1}(t) &= h_1(t_i, x_i, t_{target}, x_{target}) \\ &= (x_{target} - x_i) (t_N - t_i)^{-1}, \forall i \in \{0, 1, \dots, N-1\} \end{aligned} \quad (2.27)$$

Then

$$x(t_N) = x_{target} + \delta_N \quad (2.28)$$

and, from equation 2.26,

$$\|x_{target} - x(t_N)\| \leq \varepsilon$$

Proof:.

We have, for $i \in \{0, 1, \dots, N-1\}$,

$$\begin{aligned} u_{i,i+1} &= (x_{target} - x_i) (t_N - t_i)^{-1} \\ W_{i+1} &= x_i + u_{i,i+1} \cdot t_\varepsilon \\ x_{i+1} &= W_{i+1} + \delta_{i+1} \end{aligned}$$

Starting at $x(t_0) = x_0$,

- $i = 0$ ($t = t_0$)

$$\begin{aligned} x(t_0) &= x_0 \\ u_{0,1} &= (x_{target} - x_0) (t_N - t_0)^{-1} \\ W_1 &= x_0 + u_{0,1} t_\varepsilon \\ &= \dots \\ &= x_0 + \frac{1}{N} (x_{target} - x_0) \end{aligned}$$

- $i = 1$ ($t = t_1 = t_0 + t_\varepsilon$)

$$\begin{aligned}
x_1 &= W_1 + \delta_1 \\
u_{1,2} &= (x_{target} - x_1)(t_N - t_1)^{-1} \\
&= \dots \\
&= (x_{target} - x_0)(t_N - t_0)^{-1} - \delta_1(t_N - t_1)^{-1} \\
W_2 &= x_1 + u_{1,2}t_\varepsilon \\
&= \dots \\
&= x_0 + \frac{2}{N}(x_{target} - x_0) + \frac{N-2}{N-1}\delta_1
\end{aligned}$$

- $i = 2$ ($t = t_2 = t_0 + 2 \cdot t_\varepsilon$)

$$\begin{aligned}
x_2 &= W_2 + \delta_2 \\
u_{2,3} &= (x_{target} - x_2)(t_N - t_2)^{-1} \\
&= \dots \\
&= (x_{target} - x_0)(t_N - t_0)^{-1} - \delta_1(t_N - t_1)^{-1} - \delta_2(t_N - t_2)^{-1} \\
W_3 &= x_2 + u_{2,3}t_\varepsilon \\
&= \dots \\
&= x_0 + \frac{3}{N}(x_{target} - x_0) + \frac{N-3}{N-1}\delta_1 + \frac{N-3}{N-2}\delta_2
\end{aligned}$$

- ...

For the i -th iteration, we have

$$u_{i,i+1} = (x_{target} - x_0)(t_N - t_0)^{-1} - \sum_{k=1}^i \delta_k(t_N - t_k)^{-1} \quad (2.29)$$

and

$$W_{i+1} = x_0 + \frac{i+1}{N}(x_{target} - x_0) + \sum_{k=1}^i \frac{N-(i+1)}{N-k}\delta_k \quad (2.30)$$

with $i \in \{0, 1, \dots, N-1\}$. Recalling the solution to the system equation (equation 2.5), the position at $t = t_N$ will be

$$\begin{aligned}
x(t_N) &= x_0 + \sum_{i=0}^{N-1} (u_{i,i+1}t_\varepsilon + \delta_{i+1}) \\
&= x_0 + \sum_{i=0}^{N-1} u_{i,i+1}t_\varepsilon + \sum_{i=1}^N \delta_i
\end{aligned} \quad (2.31)$$

The second term on the right hand side of the equation can be rewritten as

$$\sum_{i=0}^{N-1} u_{i,i+1} t_\varepsilon = \sum_{i=0}^{N-1} ((x_{target} - x_0) (t_N - t_0)^{-1} - g(i)) t_\varepsilon$$

where

$$g(i) = \begin{cases} 0, & \text{if } i = 0 \\ \sum_{j=1}^i \delta_j (t_N - t_j)^{-1}, & \text{if } i > 0 \end{cases}$$

and since $t_i = t_0 + i \cdot t_\varepsilon$ (equation 2.23),

$$g(i) = \begin{cases} 0, & \text{if } i = 0 \\ \sum_{j=1}^i \delta_j ((N - j)t_\varepsilon)^{-1}, & \text{if } i > 0 \end{cases}$$

Then

$$\begin{aligned} \sum_{i=0}^{N-1} u_{i,i+1} t_\varepsilon &= \sum_{i=0}^{N-1} (x_{target} - x_0) \frac{t_\varepsilon}{t_N - t_0} - \sum_{i=0}^{N-1} g(i) t_\varepsilon \\ &= (x_{target} - x_0) \frac{N \cdot t_\varepsilon}{t_N - t_0} - \sum_{i=1}^{N-1} g(i) t_\varepsilon \\ &= x_{target} - x_0 - \sum_{i=1}^{N-1} \sum_{j=1}^i \delta_j \frac{t_\varepsilon}{(N - j)t_\varepsilon} \\ &= x_{target} - x_0 - \left(\sum_{j=1}^1 \delta_j \frac{1}{N - j} + \sum_{j=1}^2 \delta_j \frac{1}{N - j} + \dots + \sum_{j=1}^{N-1} \delta_j \frac{1}{N - j} \right) \\ &= x_{target} - x_0 - \left((N - 1) \delta_1 \frac{1}{N - 1} + (N - 2) \delta_2 \frac{1}{N - 2} + \dots + \delta_{N-1} \right) \\ &= x_{target} - x_0 - \sum_{i=1}^{N-1} \delta_i \end{aligned}$$

Replacing in equation 2.31, we get

$$\begin{aligned} x_N &= x_0 + \left(x_{target} - x_0 - \sum_{i=1}^{N-1} \delta_i \right) + \sum_{i=1}^N \delta_i \\ &= x_{target} + \delta_N \end{aligned}$$

and the distance to the target at time $t = t_N$ will be

$$\begin{aligned} \|x_N - x_{target}\| &= \|x_{target} + \delta_N - x_{target}\| \\ &= \|\delta_N\| \\ &\leq \varepsilon \end{aligned}$$

■

These results, though useful, do not state any conditions regarding their applicability, i.e, under what conditions is the target reachable using $h_1(\cdot)$ as the control strategy. For a target to be reachable, it is necessary that the control strategy used does not result in inadmissible control signals, so we turn to derive such conditions by analyzing whether $u(t) \in \mathcal{U}$ from t_0 to t_N . We do this using a worst-case approach to the external disturbances, thus deriving a sufficient, but not necessary condition.

Recall equation 2.27. Let δ_i be equal to δ^* :

$$\begin{aligned}\delta^* &= -(x_{target} - x_0) \frac{\gamma \cdot t_\epsilon}{\|x_{target} - x_0\|} \\ &= -(x_{target} - x_0) \frac{\epsilon}{\|x_{target} - x_0\|}\end{aligned}$$

for all $i \in \{1, 2, \dots, N\}$. It is easy to see that this definition of δ^* corresponds to the worst case scenario, as δ^* has a direction opposite to $u_{i,i+1}$ for all $i \in \{0, 1, \dots, N-1\}$. The norm of the corresponding control signal can be expressed as

$$\begin{aligned}\|u_{i,i+1}\| &= \left\| (x_{target} - x_0)(t_N - t_0)^{-1} - \sum_{k=1}^i \delta_k(t_N - t_k)^{-1} \right\| \\ &= \left\| (x_{target} - x_0)(t_N - t_0)^{-1} + \delta^* \sum_{k=1}^i (t_N - t_k)^{-1} \right\| \\ &= \|x_{target} - x_0\| (t_N - t_0)^{-1} + \|\delta^*\| \sum_{k=1}^i (t_N - t_k)^{-1} \\ &= \|x_{target} - x_0\| (t_N - t_0)^{-1} + \gamma t_\epsilon \sum_{k=1}^i (t_N - t_k)^{-1}\end{aligned}$$

With the control signal norm increasing monotonically with i , it will achieve its maximum for $i = N - 1$:

$$\begin{aligned}\|u_{i,i+1}\| &= \|x_{target} - x_0\| (t_N - t_0)^{-1} + \gamma t_\epsilon \sum_{k=1}^{N-1} (N - k)^{-1} t_\epsilon^{-1} \\ &= \|x_{target} - x_0\| (t_N - t_0)^{-1} + \gamma \sum_{k=1}^{N-1} (N - k)^{-1} \\ &= \|x_{target} - x_0\| (t_N - t_0)^{-1} + \gamma \sum_{k=1}^{N-1} (k)^{-1} \\ &= \|x_{target} - x_0\| (t_N - t_0)^{-1} + \gamma H_{N-1}\end{aligned}$$

where H_k denotes the k -th harmonic number. Thus the target is reachable if

$$\|x_{target} - x_0\| (t_N - t_0)^{-1} + \gamma H_{N-1} \leq u_{max}$$

Again, this is just a sufficient condition, not necessary - a consequence of the worst case considerations we have made. We sum up this result in the following condition:

Condition 2 (Reachability condition for control strategy $h_1(\cdot)$) *A sufficient condition for target reachability is*

$$\|x_{target} - x_0\| (t_N - t_0)^{-1} + \gamma \cdot H_{N-1} \leq u_{max} \quad (2.32)$$

where H_k is the k -th harmonic number,

$$H_k = \sum_{i=1}^k \frac{1}{i} \quad (2.33)$$

From proving theorem 1, we know that the control signal can also be expressed as

$$u_{i,i+1} = (x_{target} - x_0) (t_N - t_0)^{-1} - \sum_{k=1}^i \delta_k (t_N - t_i)^{-1}$$

Looking at the expression above we see that the control strategy uses the remaining time to compensate for each position drift: $[t_1, t_{target}]$ to compensate for δ_1 , $[t_2, t_{target}]$ for δ_2 , ..., $[t_i, t_N]$ for δ_i , so while traveling from x_{N-1} to x_N the agent is (still) compensating all the position drifts up until δ_{N-1} . This may become a problem if $\omega(t)$ has a non-zero mean (which is a fairly realistic scenario), possibly resulting in an increasing $\|u_{i,i+1}\|$.

2.3.6 The $h_2(\cdot)$ control strategy

A better choice would be to compensate for δ_i in while traveling from x_{i+1} to x_{i+2} , which would, in certain cases, be much less demanding on $\|u\|$ - a control strategy which we call $h_2(\cdot)$. The results for it follow:

Theorem 2 (Target reachability using control strategy $h_2(\cdot)$) *Let*

$$\begin{aligned} u_{i,i+1}(t) &= h_2(\delta_i, t_{target}, x_{target}) \\ &= (x_{target} - x_0) (t_N - t_0)^{-1} - \delta_i t_e^{-1}, \forall i \in \{0, 1, \dots, N-1\} \end{aligned} \quad (2.34)$$

Then

$$x(t_N) = x_{target} + \delta_N \quad (2.35)$$

and, from equation 2.26,

$$\|x_{target} - x(t_N)\| \leq \varepsilon$$

Proof:.

We have, for $i \in \{0, 1, \dots, N-1\}$,

$$u_{i,i+1} = (x_{target} - x_0)(t_N - t_0)^{-1} - \delta_i t_\varepsilon^{-1}$$

$$W_{i+1} = x_i + u_{i,i+1} \cdot t_\varepsilon$$

$$x_{i+1} = W_{i+1} + \delta_{i+1}$$

- $i = 0, (t = t_0)$

$$x(t_0) = x_0$$

$$u_{0,1} = (x_{target} - x_0)(t_N - t_0)^{-1} W_1 = x_0 + u_{0,1} t_\varepsilon$$

$$= \dots$$

$$= x_0 + \frac{1}{N} (x_{target} - x_0)$$

- $i = 1, (t = t_1 = t_0 + t_\varepsilon)$

$$x_1 = W_1 + \delta_1$$

$$u_{1,2} = (x_{target} - x_0)(t_N - t_0)^{-1} - \delta_1 t_\varepsilon^{-1} W_2 = x_1 + u_{1,2} t_\varepsilon$$

$$= \dots$$

$$= x_0 + \frac{2}{N} (x_{target} - x_0)$$

- $i = 2, (t = t_2 = t_0 + 2 \cdot t_\varepsilon)$

$$x_2 = W_2 + \delta_2$$

$$u_{2,3} = (x_{target} - x_0)(t_N - t_0)^{-1} - \delta_2 t_\varepsilon^{-1} W_3 = x_2 + u_{2,3} t_\varepsilon$$

$$= \dots$$

$$= x_0 + \frac{3}{N} (x_{target} - x_0)$$

- ...

For the i -th iteration, we have

$$u_{i,i+1} = (x_{target} - x_0)(t_N - t_0)^{-1} - \delta_i t_\varepsilon^{-1} \tag{2.36}$$

and

$$W_{i+1} = x_0 + \frac{i+1}{N} (x_{target} - x_0) \quad (2.37)$$

with $i \in \{0, 1, \dots, N-1\}$. Recalling equation 2.5, the position at $t = t_N$ will be

$$\begin{aligned} x(t_N) &= x_0 + \sum_{i=0}^{N-1} (u_{i,i+1} t_\varepsilon + \delta_{i+1}) \\ &= x_0 + \sum_{i=0}^{N-1} u_{i,i+1} t_\varepsilon + \sum_{i=1}^N \delta_i \\ &= x_0 + \sum_{i=0}^{N-1} ((x_{target} - x_0) (t_N - t_0)^{-1} - \delta_i t_\varepsilon^{-1}) t_\varepsilon + \sum_{i=1}^N \delta_i \\ &= x_0 + (x_{target} - x_0) \sum_{i=0}^{N-1} \frac{t_\varepsilon}{t_N - t_0} - \sum_{i=0}^{N-1} \delta_i + \sum_{i=1}^N \delta_i \\ &= x_0 + (x_{target} - x_0) \sum_{i=0}^{N-1} \frac{t_\varepsilon}{N \cdot t_\varepsilon} + \delta_N \\ &= x_0 + (x_{target} - x_0) \sum_{i=0}^{N-1} \frac{1}{N} + \delta_N \\ &= x_{target} + \delta_N \end{aligned}$$

The distance to the target at time $t = t_N$ will be

$$\begin{aligned} \|x_N - x_{target}\| &= \|x_{target} + \delta_N - x_{target}\| \\ &= \|\delta_N\| \\ &\leq \varepsilon \end{aligned}$$

■

Just as we did for theorem 1, we now derive conditions on the applicability of 2, using the same reasoning as before. Recall equation 2.34. Let δ_k be defined in the same way as it was in the previous derivation. We have

$$\begin{aligned} \|u_{i,i+1}\| &= \left\| (x_{target} - x_0) (t_N - t_0)^{-1} + \delta^* t_\varepsilon^{-1} \right\| \\ &= \|(x_{target} - x_0)\| (t_N - t_0)^{-1} + \|\delta^*\| t_\varepsilon^{-1} \\ &= \|(x_{target} - x_0)\| (t_N - t_0)^{-1} + \gamma \end{aligned}$$

So the target is reachable if

$$\|(x_{target} - x_0)\| (t_N - t_0)^{-1} + \gamma \leq u_{max} \quad (2.38)$$

Condition 3 (Reachability condition for control strategy $h_2(\cdot)$) A sufficient condition for target reachability is

$$\|x_{target} - x_0\| (t_N - t_0)^{-1} + \gamma \leq u_{max} \quad (2.39)$$

2.3.7 Comparative analysis of $h_1(\cdot)$ and $h_2(\cdot)$

While devising the $h_2(\cdot)$ control strategy with the goal of obtaining an improved version of $h_1(\cdot)$, we see that we successfully obtained a more relaxed reachability condition when compared to $h_1(\cdot)$'s. However, it should be stressed out that this does not equal improved performance, as this result (in short $\max(\|u = h_1(\cdot)\|) > \max(\|u = h_2(\cdot)\|)$) was obtained based on a particular assumption regarding the external disturbance. Still, looking at equations 2.29 and 2.36, it is clear that $h_2(\cdot)$ will yield better results when the mean disturbance has a component opposite to the direction of motion (that is, the direction pointing from the agent to the target).

We define the mean value of the control signal as

$$\bar{u} = \frac{1}{N} \sum_{i=0}^{N-1} u_{i,i+1} \quad (2.40)$$

Replacing $u_{i,i+1}$ in the equation above by eq.2.29 yields

$$\begin{aligned} \bar{u} &= \frac{1}{N} \sum_{i=0}^{N-1} \left((x_{target} - x_0) (t_N - t_0)^{-1} - \sum_{k=1}^i \delta_k (t_N - t_k)^{-1} \right) \\ &= (x_{target} - x_0) (t_N - t_0)^{-1} - \frac{1}{N} \sum_{i=0}^{N-1} \left(\sum_{k=1}^i \delta_k (t_N - t_k)^{-1} \right) \\ &= (x_{target} - x_0) (t_N - t_0)^{-1} - \frac{1}{N} \sum_{i=0}^{N-1} \left(\sum_{k=1}^i \delta_k (N - k)^{-1} t_\epsilon^{-1} \right) \\ &= (x_{target} - x_0) (t_N - t_0)^{-1} - \frac{1}{N \cdot t_\epsilon} \sum_{i=0}^{N-1} \left(\sum_{k=1}^i \delta_k (N - k)^{-1} \right) \end{aligned}$$

The last term on the right-hand side of the equation can be simplified:

$$\begin{aligned} \sum_{i=0}^{N-1} \left(\sum_{k=1}^i \delta_k (N - k)^{-1} \right) &= \sum_{i=1}^{N-1} \left(\sum_{k=1}^i \delta_k (N - k)^{-1} \right) \\ &= (\delta_1 (N - 1)^{-1}) + (\delta_1 (N - 1)^{-1} + \delta_2 (N - 2)^{-1}) + \dots + \\ &+ (\delta_1 (N - 1)^{-1} + \delta_2 (N - 2)^{-1} + \dots + \delta_{N-1} (N - (N - 1))^{-1}) \\ &= \delta_1 + \delta_2 + \dots + \delta_{N-1} \\ &= \sum_{i=1}^{N-1} \delta_i \end{aligned}$$

Then

$$\begin{aligned}
\bar{u} &= (x_{target} - x_0) (t_N - t_0)^{-1} - \frac{1}{N \cdot t_\epsilon} \sum_{i=1}^{N-1} \delta_i \\
&= (x_{target} - x_0) (t_N - t_0)^{-1} - \frac{1}{N} \sum_{i=1}^{N-1} \bar{\omega}_i \\
&= (x_{target} - x_0) (t_N - t_0)^{-1} - \frac{N-1}{N} \bar{\omega}
\end{aligned} \tag{2.41}$$

where $\bar{\omega}$ is the mean disturbance from t_0 to t_{target} .

As for $h_2(\cdot)$, we have:

$$\begin{aligned}
\bar{u} &= \frac{1}{N} \sum_{i=0}^{N-1} ((x_{target} - x_0) (t_N - t_0)^{-1} - \delta_i t_\epsilon^{-1}) \\
&= (x_{target} - x_0) (t_N - t_0)^{-1} - \frac{1}{N} \sum_{i=1}^{N-1} (\delta_i t_\epsilon^{-1}) \\
&= (x_{target} - x_0) (t_N - t_0)^{-1} - \frac{1}{N} \sum_{i=1}^{N-1} (\bar{\omega}_i) \\
&= (x_{target} - x_0) (t_N - t_0)^{-1} - \frac{N-1}{N} \bar{\omega}
\end{aligned} \tag{2.42}$$

As it should be expected, the mean control signals are the same for both control signals. So, other than the peak values, in what else do the control strategies differ? The answer to this comes from equations 2.30 and 2.37 - the waypoint positions. In the latter, the waypoints will always lie somewhere along the ideal trajectory, as opposed to the former, which is more sensitive to disturbances.

2.3.8 The final approach

Independent of the control strategy used, at this point ($t = t_N$) the agent is at most ϵ meters away from the target with t_f seconds. Again picking up on the principle behind equation 2.8, we devise the control strategy for the final approach

Theorem 3 (Target reachability (Final approach)) *Let*

$$x(t_N) = x_{target} + \delta_N$$

Setting

$$u_f(t) = -\delta_N \cdot t_f^{-1} \tag{2.43}$$

results in

$$\begin{aligned} W_f &= x_N + u_f \cdot t_f \\ &= x_{target} \end{aligned} \quad (2.44)$$

and

$$\begin{aligned} x_f &= x_N + u_f \cdot t_f + \int_{t_N}^{t_{target}} w(t) dt \\ &= x_{target} + \delta_f \end{aligned} \quad (2.45)$$

Consequently,

$$\|x_f - x_{target}\| \leq \gamma \cdot t_f \quad (2.46)$$

Proof.:

At this point, we have t_f seconds left to reach the target, so we can set

$$\begin{aligned} u_f &= \delta_N(t_f)^{-1} \\ W_f &= x_N + u_f t_f \\ &= x_{target} \end{aligned}$$

to have

$$x(t_{target}) = x_{target} + \delta_f$$

Knowing that $\|\delta\| \leq \gamma \cdot t$, the distance to the target at $t = t_{target}$ will be

$$\begin{aligned} \|x(t_{target}) - x_{target}\| &= \|x_{target} + \delta_f - x_{target}\| \\ &= \|\delta_f\| \\ &\leq \gamma \cdot t_f \end{aligned}$$

■

2.4 Clock drift

Before leaving the single vehicle scenario, we consider the case where the agent's clock isn't completely accurate, in what we call clock drift. Here, we assume there is a difference of τ

seconds between the agent's clock and the reference time

$$t_{i+1}^{agent} = t_{i+1}^{ref.} + \tau$$

counting from the last *departure* instant, t_i , as it is assumed the clocks were synchronized ($t_i^{agent} = t_i^{ref.}$) at that instant:

$$\begin{aligned} t_{i+1}^{agent} &= t_i^{ref.} + t_\varepsilon + \tau \\ &= t_i^{agent} + t_\varepsilon + \tau \end{aligned}$$

Thus, $\tau > 0$ corresponds to a time lag and the opposite to a lead. Since the control law is applied for a different time than it should, the expected (i.e., ideal) stopping point will also be different:

$$\begin{aligned} W_{i+1}^\tau &= x_i + u_{i,i+1}(t) \cdot (t_{i+1}^{agent} - t_i^{agent}) \\ &= x_i + u_{i,i+1}(t) \cdot (t_\varepsilon + \tau) \\ &= W_{i+1} + u_{i,i+1}(t)\tau \end{aligned}$$

Of course, clock drift will also have implications on the uncertainty set. Having defined the uncertainty set at time t_{i+1} as the circle of radius $\gamma(t_{i+1} - t_i)$ centered around the ideal position at time t_{i+1} , $x(t_{i+1})$, a drift of τ seconds will result in a scaling of the uncertainty set by $(1 + \frac{\tau}{t_\varepsilon})$, as the radius of $\Delta(t_{i+1}^{agent})$ is equal to $\gamma(t_{i+1}^{agent} - t_i^{agent})$ or, simply put, $\gamma(t_\varepsilon + \tau)$.

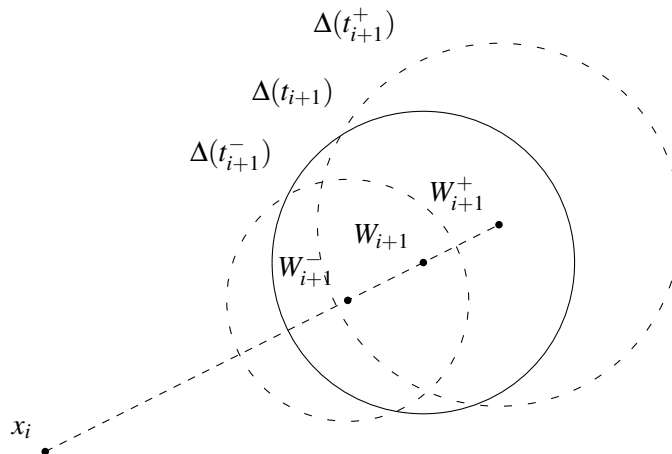


Figure 2.6: The effects of clock drift in the ideal stopping position and the uncertainty set. The superscript "+" denotes a time lag ($\tau > 0$) and the superscript "-" to a time lead ($\tau < 0$).

Chapter 3

Multiple agents

Having devised an approach to the single agent problem, we now turn to the multiple agent scenario. Here, we have a set of M agents, $A = \{a_1, a_2, \dots, a_M\}$, which we want to drive from the set of initial positions $X_0 = \{x_0^1, x_0^2, \dots, x_0^M\}$ to the set of target positions, $X_{target} = \{x_{target}^1, x_{target}^2, \dots, x_{target}^M\}$. Assuming we are dealing with a formation, it is also desirable to maintain the relative positions between agents, described by the elements $c_{i,j}$ of $C \in \mathbb{R}^{M \times M}$. Finally, a key aspect of (mobile) multi-agent networks is that of connectivity: we want to keep the network connected as the failure to do so may result in the loss of one or more agents.

3.1 Background

Before dealing with the multi-agent problem itself, we recall some important concepts and definitions from graph theory [8].

3.1.1 Graph Theory

Definition 7 (Graph) A graph $G = \{N, E\}$ is defined by a set of nodes, N , and a set E of edges, connecting the nodes in N . The order of a graph G is simply the number of nodes it contains, n , whereas its size is the number e of edges in E .

Definition 8 (Path) A path is a sequence of nodes such that for any two consecutive nodes $i, i+1$ in the path, $\{i, i+1\} \in E$.

Definition 9 (Neighborhood) The neighborhood of a node n_i is the set of its adjacent nodes, that is, the nodes that are connected to n_i by an edge.

Definition 10 (Connected graph) *A graph in which, given any two nodes, there is always a path connecting them, is said to be connected.*

Definition 11 (Connected component) *A connected component of a graph G is a maximal connected subgraph of G . A connected graph has only one connected component.*

Definition 12 (Adjacency matrix) *The adjacency matrix A is a way to represent a graph G . It is a n -by- n matrix, where*

$$a_{i,j} = \begin{cases} 1, & \text{if } \{i, j\} \in E \\ 0, & \text{otherwise} \end{cases} \quad (3.1)$$

As we are dealing with undirected graphs, A will be symmetric.

Definition 13 (Degree matrix) *The degree matrix D is a n -by- n diagonal matrix where the element $d_{i,i}$ is the degree of the i -th node (the number of edges incident on the node - loops are counted twice).*

Definition 14 (Laplacian matrix) *The Laplacian matrix is another way to represent a graph, and it is defined as the difference between the degree and adjacency matrices:*

$$L = D - A \quad (3.2)$$

We are interested in a special property of the Laplacian matrix: the number of connected components in G is equal to the number of eigenvalues that are zero (note that since L is positive semi-definite, $\lambda_i \geq 0$).

Although important, we are interested in most of these concepts from a simulation perspective, as they are essential to algorithms for detecting the loss of one or more agents, or passing waypoints from the leader to the rest of the network.

3.1.2 Connectivity

As we have already mentioned, we are interested in keeping the network connected, so as to preventing agents from being lost. Inter-agent connectivity is then modeled as a simple matter of range - only when agent i is within agent j 's communication range are the two able to communicate directly - in other words, $\{a_i, a_j\} \in E$. This range parameter, r , is assumed to be the same for all agents, for the sake of simplicity.

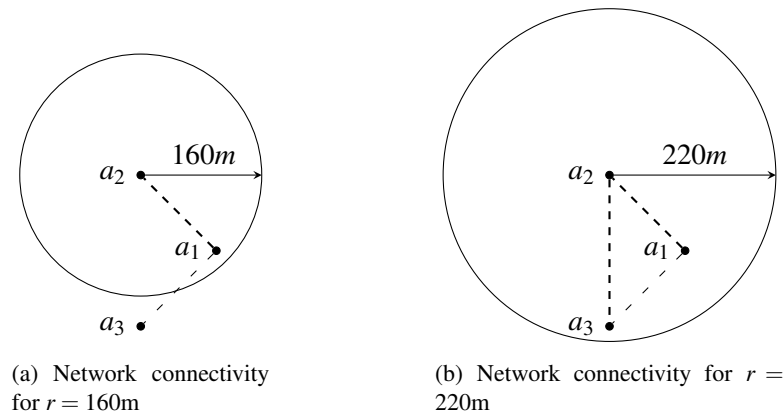


Figure 3.1: Network connectivity for different communication ranges.

3.2 A two-agent network

We begin by studying a simple, two-agent network, where we let one of them (the leader, a_L) "behave" as in the single agent scenario, with the difference that it must inform the other agent about *where* it is going to go next - the next waypoint - as well as *when* it plans to get there - the travel time.

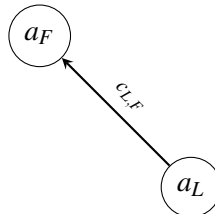


Figure 3.2: A two agent network

3.2.1 Waypoint definition

This agent (the follower, a_F), which supposed to be synchronized with the leader at all times, makes use that information to determine its own waypoint. The travel time (more specifically, the departure and arrival times), however, is required to be the same as the leader's, otherwise the agent will not have access to the leader's information and will consequently be lost. Thus synchronization is a key to success, but is not enough to guarantee success, for a follower failing to be inside the leader's communication range at one of the stopping instants will also result in agent loss.

We define the initial and target sets by $X_0 = \{x_0^L, x_0^F\}$ and $X_{target} = \{x_{target}^L, x_{target}^F\}$ respectively. Since the network is also a formation, it is natural to assume that $x_0^F = x_0^L + c_{L,F}$ and $x_{target}^F = x_{target}^L + c_{L,F}$. In fact, as the inter-agent relative position is to be maintained, we use this to determine the follower's waypoint:

$$W_{k+1}^F = W_{k+1}^L + c_{L,F} \quad (3.3)$$

3.2.2 Reaching the target

Assuming the follower is successful in keeping within the leader's communication range at all the relevant instants¹, we are interested in knowing $x^F(t_N)$ ² or, in other words, x_N^F . From the solution to the single agent problem (equations 2.5, 2.31 and 2.38), we know that this is given by

$$x^F(t_N) = x_0^F + \sum_{k=0}^{N-1} u_{k,k+1}^F \cdot t_\epsilon + \sum_{k=1}^N \delta_k^F \quad (3.4)$$

Looking at the expression above, we need to determine $u_{k,k+1}^F$. We can use equation 3.3 to obtain

$$\begin{aligned} u_{k,k+1}^F &= (W_{k+1}^F - x_k^F) t_\epsilon^{-1} \\ &= (W_{k+1}^L + c_{L,F} - x_k^F) t_\epsilon^{-1} \end{aligned}$$

Recalling equation 2.25

$$\begin{aligned} u_{k,k+1}^F &= (W_{k+1}^L + c_{L,F} - (W_k^F + \delta_k^F)) t_\epsilon^{-1} \\ &= (W_{k+1}^L + c_{L,F} - W_k^F - \delta_k^F) t_\epsilon^{-1} \\ &= (W_{k+1}^L + c_{L,F} - (W_k^L + c_{L,F}) - \delta_k^F) t_\epsilon^{-1} \\ &= (W_{k+1}^L - W_k^L - \delta_k^F) t_\epsilon^{-1} \\ &= (W_{k+1}^L - (x_k^L - \delta_k^L) - \delta_k^F) t_\epsilon^{-1} \\ &= (W_{k+1}^L - x_k^L + \delta_k^L - \delta_k^F) t_\epsilon^{-1} \\ &= (W_{k+1}^L - x_k^L) t_\epsilon^{-1} + (\delta_k^L - \delta_k^F) t_\epsilon^{-1} \\ &= u_{k,k+1}^L + (\delta_k^L - \delta_k^F) t_\epsilon^{-1} \end{aligned} \quad (3.5)$$

¹We will deal with this assumption with greater detail further ahead.

²Recall that $t_{target} = t_N + t_f = N \cdot t_\epsilon + t_f$, with $t_f \leq t_\epsilon$

We are now able to replace $u_{k,k+1}^F$ in equation 3.4 by 3.5:

$$\begin{aligned}
x^F(t_N) &= x_0^F + \sum_{k=0}^{N-1} (u_{k,k+1}^L + (\delta_k^L - \delta_k^F) t_\varepsilon^{-1}) t_\varepsilon + \sum_{k=1}^N \delta_k^F \\
&= x_0^F + \sum_{k=0}^{N-1} u_{k,k+1}^L t_\varepsilon + \sum_{k=0}^{N-1} \delta_k^L - \sum_{k=0}^{N-1} \delta_k^F + \sum_{k=1}^N \delta_k^F \\
&= x_0^F + \sum_{k=0}^{N-1} u_{k,k+1}^L t_\varepsilon + \sum_{k=1}^{N-1} \delta_k^L - \sum_{k=1}^{N-1} \delta_k^F + \sum_{k=1}^N \delta_k^F \\
&= x_0^F + \sum_{k=0}^{N-1} u_{k,k+1}^L t_\varepsilon + \sum_{k=1}^{N-1} \delta_k^L + \delta_N^F
\end{aligned} \tag{3.6}$$

To find $x^F(t_N)$, we have to solve equation 3.6 for each control strategy, that is, $u_{k,k+1}^L = h_1(\cdot)$ and $u_{k,k+1}^F = h_2(\cdot)$

3.2.2.1 $h_1(\cdot)$

From proving target reachability using $h_1(\cdot)$ in the single agent scenario, we know that (eq. 2.31)

$$x_0^L + \sum_{k=0}^{N-1} u_{k,k+1}^L t_\varepsilon + \sum_{k=1}^N \delta_k^L = x_{target}^L + \delta_N^L$$

Replacing in 3.6 yields

$$\begin{aligned}
x^F(t_N) &= x_0^F + \left(x_{target}^L + \delta_N^L - x_0^L - \sum_{k=1}^N \delta_k^L \right) + \sum_{k=1}^{N-1} \delta_k^L + \delta_N^F \\
&= x_{target}^L + x_0^F - x_0^L - \sum_{k=1}^N \delta_k^L + \delta_N^L + \sum_{k=1}^{N-1} \delta_k^L + \delta_N^F \\
&= x_{target}^L + c_{L,F} - \sum_{k=1}^N \delta_k^L + \sum_{k=1}^N \delta_k^L + \delta_N^F \\
&= x_{target}^F + \delta_N^F
\end{aligned} \tag{3.7}$$

3.2.2.2 $h_2(\cdot)$

Replacing $u_{k,k+1}^L$ in equation 3.5 by equation 2.34 yields

$$\begin{aligned}
u_{k,k+1}^F &= (\delta_k^L - \delta_k^F) t_\varepsilon^{-1} + (x_{target}^F t_N^{-1} - \delta_k^L t_\varepsilon^{-1}) \\
&= x_{target}^F t_N^{-1} - \delta_k^F t_\varepsilon^{-1}
\end{aligned} \tag{3.8}$$

so the follower sets its speed exactly in the same way as the leader. Because of that, the proof we have used for target reachability using $h_2(\cdot)$ in the single agent problem can also be used to show

that the follower reaches its target, with its final position being

$$x^F(t_N) = x_{target}^F + \delta_N^F \quad (3.9)$$

As we can see from equations 3.7 and 3.9, the position of the following agent is the same, regardless of the control strategy used by the leader. And since $\delta \leq \varepsilon$

$$\|x^F(t_N) - x_{target}^F\| \leq \varepsilon \quad (3.10)$$

the upper bound on the distance to the target at the end of the main approach is the same for both leader and follower.

3.2.3 Inter-agent distance

So far we have assumed the follower to be able to keep close enough to the leader, so as to be able to be informed of the next waypoint. As such, we are only interested in the distance between the two agents when they are about to communicate, which only happens at the stopping instants t_k

$$\begin{aligned} \|x^L(t_k) - x^F(t_k)\| &= \|x_k^L - x_k^F\| \\ &= \|(W_k^L + \delta_k^L) - (W_k^F + \delta_k^F)\| \\ &= \|W_k^L + \delta_k^L - (W_k^L + c_{L,F}) - \delta_k^F\| \\ &= \|\delta_k^L - \delta_k^F - c_{L,F}\| \end{aligned}$$

Knowing that $\|\delta_k\| \leq \varepsilon$ for any of the two agents if the disturbance set is the same for both, we can let

$$\begin{aligned} \delta_k^L &= -\delta_k^F \\ &= -\frac{\varepsilon}{\|c_{L,F}\|} c_{L,F} \end{aligned}$$

and obtain the following upper bound on the inter-agent distance

$$\begin{aligned} \|x_k^L - x_k^F\| &\leq \left\| -\frac{\varepsilon}{\|c_{L,F}\|} c_{L,F} - \frac{\varepsilon}{\|c_{L,F}\|} c_{L,F} - c_{L,F} \right\| \\ &\leq 2\varepsilon + \|c_{L,F}\| \end{aligned} \quad (3.11)$$

3.2.3.1 Conditions on ε

Bearing in mind we want to keep connectivity between the two agents, the following condition should hold:

$$r \geq 2\varepsilon + \|c_{L,F}\|$$

or, alternatively,

$$\varepsilon \leq \frac{1}{2}(r - \|c_{L,F}\|) \quad (3.12)$$

In obtaining the previous upper bound on the inter-agent distance, we let the two agents drift apart in the direction of $c_{L,F}$. If we now let them drift closer to each other in the same direction, it would take them $\frac{1}{2}\|c_{L,F}\|\gamma^{-1}$ seconds to reach the same position ($x^L(t) = x^F(t)$) - in other words, the two agents would take that amount of time to collide with each other. As such, we require that the vehicles travel for a time smaller than that, or else we cannot guarantee that they will not collide.

$$t_\varepsilon < \frac{1}{2}\|c_{L,F}\|\gamma^{-1}$$

and since $t_\varepsilon = \varepsilon\gamma^{-1}$,

$$\varepsilon < \frac{1}{2}\|c_{L,F}\| \quad (3.13)$$

With equations 3.12 and 3.13 we have obtained two conditions on ε to keep the agents from both colliding and drifting too far apart.

3.3 The multi-agent network

After obtaining some results for the two-agent network, we finally move on to the more general network, where we now have a set of agents $A = \{a_1, a_2, \dots, a_M\}$ as well as the initial and target sets, $X_0 = \{x_0^1, x_0^2, \dots, x_0^M\}$ and $X_{target} = \{x_{target}^1, x_{target}^2, \dots, x_{target}^M\}$. We will, however, keep some aspects of the two-agent network, such as the presence of a leader (in other words, maintain a centralized approach), and the use of the formation property of the network to define waypoints.

3.3.1 Waypoint definition

Again, we assign one agent, a_1 , the task of leading the network to the target set, which it does by computing its next waypoint and then transmitting it to the rest of the network. Here lies an issue that can't be captured by the previous network example: it is very likely that not all agents are

within the leader's communication range, that is, $\mathcal{N}(a_1) \subset A$, so the waypoint mechanism has to be a little more complex.

Broadcasting

The simplest way is to have the leader transmit W_{k+1}^L to its neighborhood and all other agents (other than the leader) acting as repeaters until all agents are updated. Then, each agent just needs to add to the received waypoint its relative distance to the leader:

$$W_{k+1}^j = W_{k+1}^L + c_{L,j} \quad (3.14)$$

Spanning tree

Another alternative is to consider a spanning tree of the graph with the leader as root and then transmitting the waypoints from parent to child nodes, updating them on the way, in the same fashion as a breadth-first search on the spanning tree.:

$$W_{k+1}^j = W_{k+1}^i + c_{i,j} \quad (3.15)$$

where agent j is a child of agent i .

3.3.2 Connection to the two-agent network

Note that although the second mechanism may be, at least theoretically, more energy efficient³, the two are equivalent (will result on the same waypoints for each agent), so regardless of the one that is chosen, we have that for every agent a_j other than the leader, the $k + 1$ -th waypoint is obtained, directly or not, from the leader's:

$$W_{k+1}^j = W_{k+1}^L + c_{L,j} \quad (3.16)$$

Looking at the equation above we see that if we consider just the leader and any other agent, the "behavior" is exactly the same as for the two-agent network that we have analyzed. Doing this for all agents in the network, it is easy to see that we are able to extend the results we obtained for the two-agent network. We summarize this approach with algorithm 2.

³If, to each edge $\{a_i, a_j\}$ in the original network graph we associate the *physical* distance between agents a_i and a_j as the weight, using the minimum spanning tree obtained for waypoint transmission would *theoretically* require less transmission power.

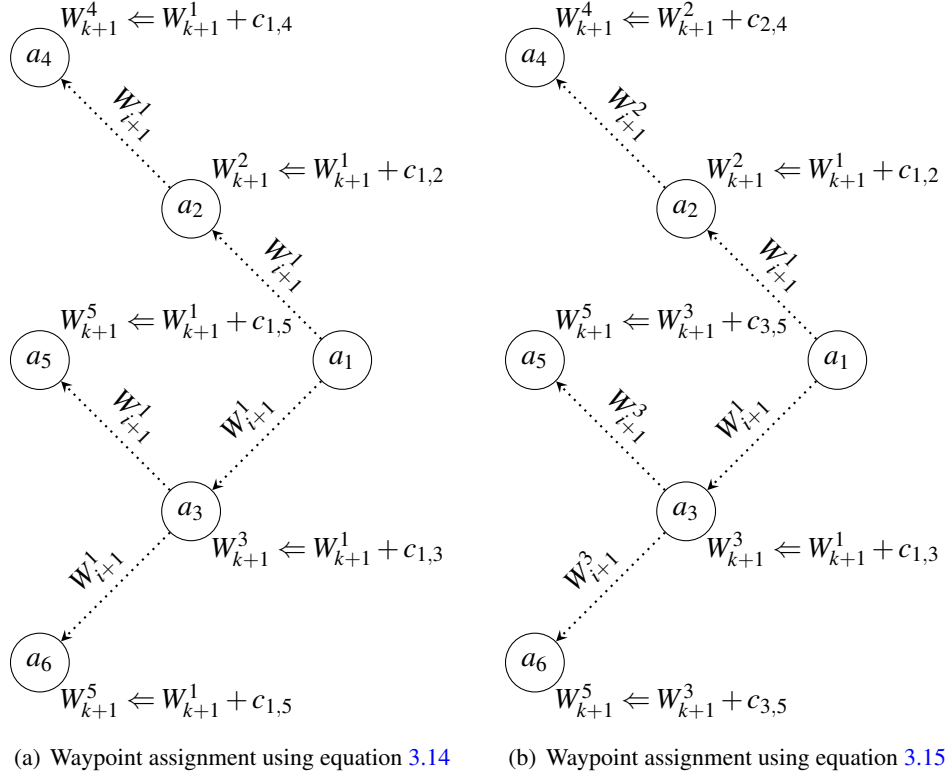


Figure 3.3: Difference between the proposed waypoint assignment/transmission mechanisms

3.3.3 Bounds and conditions

In algorithm 2 the control strategy $h(\cdot)$ is assumed to be able to drive the network to the target set without losing any agents. To prove that the proposed solution for the multi agent network is feasible, we first have to prove that this assumption holds.

When analyzing the two-agent network, we saw that having the leader use any of the control strategies proposed for the single agent case would successfully drive the network close to the target set, *if* the conditions on the inter-agent distance were met. Since we have concluded that the multi-agent network can be "reduced", in some sense, to the two-agent network, those results, although with some modifications, are also valid for the n -agent network.

The collision condition

With equation 3.13, we expressed a condition on the maximum position uncertainty (for any of the two agents in the network) needed to prevent them from colliding with each other. For M agents, however, the condition is slightly different. Consider the C matrix, expressing the desired relative

Algorithm 2 Main approach

```

1:  $t_\varepsilon \leftarrow \varepsilon \gamma^{-1}$ 
2:  $N \leftarrow \left\lfloor \frac{(t_{\text{target}} - t_0)}{t_\varepsilon} \right\rfloor$ 
3: for  $k = 0$  to  $N - 1$  do
4:    $t_{k+1} = t_k + t_\varepsilon$ 
5:    $u_{k,k+1}^1 = h(\cdot)$ 
6:    $W_{k+1}^1 = x_k + \int_{t_k}^{t_{k+1}} u_{k,k+1}^1(t) dt$ 
7:   for  $i = 2$  to  $M$  do
8:      $W_{k+1}^i = W_{k+1}^1 + c_{1,k}$ 
9:      $u_{k,k+1}^i = (W_{k+1}^i - x_k^i) t_\varepsilon^{-1}$ 
10:  end for
11:  for  $k = 1$  to  $M$  do
12:     $\delta_{k+1}^i = \int_{t_k}^{t_{k+1}} \omega^i(t) dt$  {  $\omega^i(t)$  is the external speed disturbance }
13:     $x_{k+1}^i = W_{k+1}^i + \delta_{k+1}^i$ 
14:  end for
15: end for

```

positions between the agents in the network. Defining

$$d_{i,j} = \|c_{i,j}\|, \text{ with } i \neq j \quad (3.17)$$

as the (desired) distance between agents a_i and a_j ,

$$i^*, j^* = \arg \min (d_{i,j})$$

will be the two closest agents in the network. This means that these are the two agents whose over-approximating uncertainty sets Δ_i and Δ_j (which are discs centered at the agent's estimated/ideal position) take the least amount of time to overlap. This overlap, which represents a collision possibility between the two agents, occurs when the radius of either one of the uncertainty sets exceeds half of the distance between two agents, and thus we express the collision condition as

$$\varepsilon < \frac{1}{2} \min (d_{i,j}), \text{ with } i \neq j \quad (3.18)$$

The range condition

Another condition for the two-agent network was that the two agents had to remain within the communication range of each other, which was expressed by equation 3.12. Analogously to what happened with the previous condition, there will be some changes due to the higher number of agents. Consider agent a_i , for example, in a network where every agent has a communication range equal to r . This agent has a certain set of agents within its communication range, $\mathcal{N}(i)$ to be exact. Assuming we do not want it to lose connectivity to any of these, we would write the

corresponding condition as

$$\varepsilon_i \leq \frac{1}{2} \left(r - \max_{j \in \mathcal{N}(i)} (d_{i,j}) \right)$$

which is just a slight modification of the original equation to reflect our connectivity restriction. Of course, if we want this to be true for all agents, then we express the range condition as

$$\varepsilon \leq \min_{i \in A} \left[\frac{1}{2} \left(r - \max_{j \in \mathcal{N}(i)} (d_{i,j}) \right) \right] \quad (3.19)$$

where A is the set of all agents in the network.

It should be mentioned that these conditions have all been obtained by considering worst-case scenarios and, consequently, might be overly conservative, so care should be taken when choosing the maximum position uncertainty parameter, ε .

Finally, we sum up the upper bounds on position uncertainty obtained using the control strategies initially proposed for the single agent problem.

Theorem 4 (Target set reachability using control strategy $h_1(\cdot)$) *Let*

$$\begin{aligned} u_{k,k+1}^L(t) &= h_1(x_{target}^L, x_k^L, t_N, t_k) \\ &= (x_{target}^L - x_k^L) (t_N - t_k)^{-1}, \forall k \in \{0, 1, \dots, N-1\} \end{aligned} \quad (3.20)$$

Then

$$x^i(t_N) = x_{target}^i + \delta_N^i$$

and, from equation 2.26,

$$\|x_{target}^i - x^i(t_N)\| \leq \varepsilon$$

for all $i \in \{1, 2, \dots, M\}$.

Theorem 5 (Target set reachability using control strategy $h_2(\cdot)$) *Let*

$$\begin{aligned} u_{k,k+1}^L(t) &= h_2(x_{target}^L, \delta_k^L, t_N, t_\varepsilon) \\ &= x_{target}^L \cdot t_N^{-1} - \delta_k^L \cdot t_\varepsilon^{-1}, \forall k \in \{0, 1, \dots, N-1\} \end{aligned} \quad (3.21)$$

Then

$$x^i(t_N) = x_{target}^i + \delta_N^i$$

and, from equation 2.26,

$$\|x_{target}^i - x^i(t_N)\| \leq \varepsilon$$

for all $i \in \{1, 2, \dots, M\}$.

Chapter 4

Disturbance set estimation

So far we have assumed that the disturbance set Ω is (approximately) known, or that there is enough knowledge of it to extract the upper bound γ . In order to have a more robust approach, we would like to be able to deal with the case when our knowledge of Ω is poor or even inexistent, as it is reasonable to assume that in most cases, Ω is unknown *a priori*. Consider, for example, the AUV scenario: Ω can be time-varying, as a vehicle in an open sea trajectory may go through areas with very different, oceanic currents. As such, it is better to let the agent's knowledge of Ω evolve with time rather than letting it be fixed and equal to an initial estimate. To this purpose, we use the position drifts, δ_i , to try and characterize Ω .

4.1 Background

We now face the problem of how to describe Ω , so we first have to choose what to use to approximate that set. Although ellipsoids will not, by themselves, fully describe the set, they will prove very useful.

4.1.1 Ellipsoids

An ellipsoid \mathcal{E} with center $c \in \mathbb{R}^n$ and shape matrix Q , with Q symmetric positive definite is defined by

$$\mathcal{E}(c, Q) = \{x \in \mathbb{R}^n : (x - c)^T Q^{-1} (x - c) \leq 1\} \quad (4.1)$$

The directions of the ellipsoid's axis are given by the eigenvectors of the matrix Q , with the radii given by the square root of the corresponding eigenvalue.

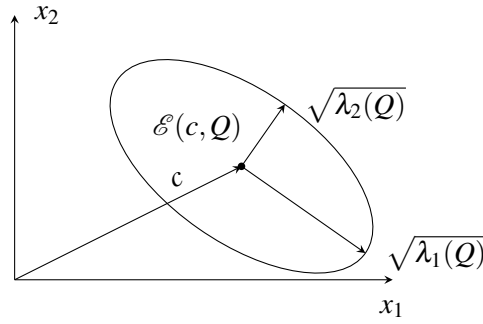


Figure 4.1: The ellipsoid $\mathcal{E}(c, Q)$. λ_1 denotes Q 's largest eigenvalue.

We choose the normal distribution to approximate the disturbance set, since not only it accurately describes underwater currents [18], but it is also general enough to approximate many relevant physically phenomena.

4.1.2 The Normal Distribution

A N -dimensional normal distribution is completely characterized by its mean μ , and variance Σ : $X \sim \mathcal{N}(\mu, \Sigma)$. In particular, for a bivariate normal distribution, the probability density function is

$$f_x(x) = \frac{1}{2\pi \det(\Sigma)^{\frac{1}{2}}} e^{-\frac{1}{2}(x-\mu)^T \Sigma^{-1}(x-\mu)} \quad (4.2)$$

where

$$\mu = \begin{bmatrix} \mu_1 \\ \mu_2 \end{bmatrix}, \Sigma = \begin{bmatrix} \sigma_{1,1}^2 & \sigma_{1,2}^2 \\ \sigma_{2,1}^2 & \sigma_{2,2}^2 \end{bmatrix}$$

An important characteristic of this distribution, regardless of its dimensionality, is that it is not bounded. Nonetheless, we know (from the *empirical rule*) that for a unidimensional normal distribution:

- 68.27% of the results are within one standard deviation of the mean,
- 95.45% of the results are within two standard deviations of the mean,
- 99.73% of the results are within three standard deviations of the mean,
- 99.99% of the results are within four standard deviations of the mean.

This can be extended¹ to the multidimensional distribution as follows:

¹For greater detail, please refer to the appendix

- 39.45% of the results lie in the ellipsoid $\mathcal{E}(\mu, \Sigma)$,
- 86.47% of the results lie in the ellipsoid $\mathcal{E}(\mu, 2^2\Sigma)$,
- 98.89% of the results lie in the ellipsoid $\mathcal{E}(\mu, 3^2\Sigma)$,
- 99.97% of the results lie in the ellipsoid $\mathcal{E}(\mu, 4^2\Sigma)$.

This result comes from the fact that the level curves - known as equidensity curves for a probability density function - for this distribution are *ellipsoids* centered at the mean μ and shape matrix $k\Sigma$, where $k \in \mathbb{R}^+$.

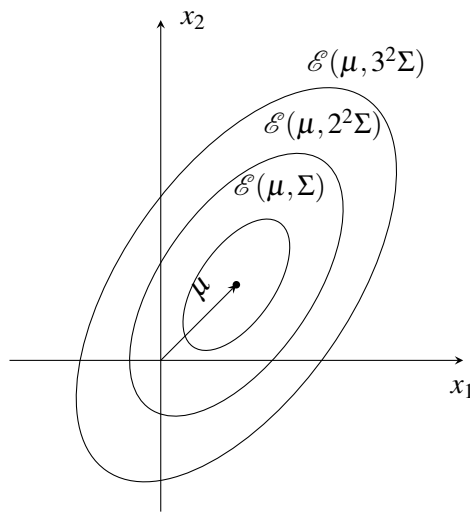


Figure 4.2: The confidence ellipsoids $\mathcal{E}(\mu, k^2\Sigma)$ for $k = \{1, 2, 3\}$.

4.2 Application to the single agent problem

Having defined what we will use to characterize the disturbance set, we now know that in order to describe Ω , we need to estimate the mean disturbance μ and the respective covariance, Σ .

4.2.1 The average disturbance

From the previous chapter we know that the i -th stopping point will be located at

$$x_i = W_i + \delta_i$$

Since both x_i and W_i are known, the position drift δ_i can be easily obtained. Moreover, as the travel time needed to go from x_{i-1} to x_i is also known, we can define the *mean* disturbance speed during

that time interval as

$$\bar{\omega}_i = \delta_i \cdot (t_i - t_{i-1})^{-1} \quad (4.3)$$

We then use this measurement, along with all the other measurements up until that instant² to estimate the mean μ

$$\mu_i = \frac{1}{i} \sum_{k=1}^i \bar{\omega}_k \quad (4.4)$$

and the covariance Σ

$$\Sigma_i = \frac{1}{i} \sum_{k=1}^i (\bar{\omega}_k - \mu_i) (\bar{\omega}_k - \mu_i)^T \quad (4.5)$$

Since these operations require a growing number of operations, we instead use their recursive counterparts:

$$\mu_i = (1 - i^{-1})\mu_{i-1} + i^{-1}\bar{\omega}_i \quad (4.6)$$

and

$$\Sigma_i = (1 - i^{-1}) \left[\Sigma_{i-1} + i^{-1} (\bar{\omega}_i - \mu_{i-1}) (\bar{\omega}_i - \mu_{i-1})^T \right] \quad (4.7)$$

4.2.2 Implications of a normally distributed disturbance set

We now pause to make some considerations on Ω : if Ω is indeed normally distributed, then, as has already been mentioned, it will no longer be bounded, as we have assumed so far - instead Ω will now be \mathbb{R}^2 . As a consequence, the uncertainty set would also be \mathbb{R}^2 , as condition 2.12 isn't met and the upper bound on the position drift expressed by equation 2.26 no longer holds. Although this puts our approach at stake, since we no longer have an upper bound on the uncertainty, we make use of the previously mentioned confidence levels to help us solve this problem.

4.2.3 Confidence levels

We define the disturbance set approximation Ω_i^1 as the ellipsoid $\mathcal{E}(\mu_i, \Sigma_i)$. From the results in the previous subsection we know that if $\mu_i \approx \mu$ and $\Sigma \approx \Sigma_i$, then this set will contain around 40% of the external disturbance values. Just as we did in the single agent problem, we then use it to define the associated uncertainty set $\Delta_i^1 = \Omega_i^1(t_i - t_{i-1})$. We now know that there is also a probability of

²The use of *all* the available measurements comes from the assumption that the number N of waypoints is such (i.e., small) that it does not justify the use of a (weighted) moving average.

k	$P[x(t_{i+1}) \in \Delta_i^k]$
1	39.45%
2^2	86.47%
3^2	98.89%
4^2	99.97%

Table 4.1: Confidence levels for the different uncertainty sets.

around 40% of the agent being inside that set:

$$P[x(t_i) \in \Delta_i^1] \approx 40\%$$

Generically, we define

$$\Omega_i^k = \mathcal{E}(\mu_i, k^2 \Sigma_i) \quad (4.8)$$

$$\Delta_i^k = (t_i - t_{i-1}) \Omega_i^k \quad (4.9)$$

Given the control signal $u_{i,i+1}$ we can, if our mean and covariance estimates are good, define the the uncertainty sets at $t = t_{i+1}$ and the associated confidence levels

4.2.4 Disturbance and uncertainty sets

We can now relate these sets with our initial approach, that is, with ε and γ .

If we take, for example, the mean and covariance estimates at time t_i , μ_i and Σ_i , and assume that these *approximately describe the true disturbance set*, we can then make some considerations regarding an upper bound on the agents's distance to the waypoint at the next stopping instant, t_{i+1} . We start with the disturbance set estimate Ω_{i+1}^k :

$$\Omega_{i+1}^1 = \mathcal{E}(\mu_i, \Sigma_i)$$

We want to find an upper bound on the disturbance speed γ which, in this case, is defined by (recall equation 2.12)

$$\gamma_i^k = \max_{\omega \in \Omega_i^k} (\|\omega\|) \quad (4.10)$$

Zero mean

If μ_i is sufficiently small, one can set

$$\gamma_i^k = \max \left(\sqrt{\lambda(\Sigma_i)} \right)$$

as the length of the major axis of the corresponding ellipsoid ($\Omega_i^k = \mathcal{E}(\mu_i, k^2 \Sigma_i)$) is equal to the square root of the largest eigenvalue of the shape matrix. This defines the corresponding over-approximating set

$$\Omega_{i(over)}^k = \{\omega \in \mathcal{R}^2 : \|\omega\| \leq \gamma\} \quad (4.11)$$

Since the over-approximated ellipsoid is a (proper) subset of $\Omega_{i(over)}^k$, then the associated probability for the over-approximating set will be at least equal to that of the ellipsoid. The same can be said for the corresponding over-approximated uncertainty set estimate

$$\delta_{i(over)}^k(t_{i+1}) = \Omega_{i(over)}^k(t_{i+1} - t_i)$$

which is a disc of radius $\gamma_i^k(t_{i+1} - t_i)$ centered at W_{i+1} . This radius is thus the upper bound on the position uncertainty or, in other words, ε^k (recall that $\varepsilon = \gamma \cdot t_\varepsilon$).

Non-zero mean

If, however, the mean disturbance isn't small enough to be disregarded, then the problem becomes less simple. Finding the norm of the largest disturbance in Ω_i^k is, in geometric terms, the equivalent of finding the minimum bounding circle centered at the origin for the ellipsoid $\mathcal{E}(\mu_i, k^2 \Sigma_i)$ - a simple problem if the ellipsoid is also centered at the origin. This can be formulated as

$$\begin{aligned} \gamma_i^k &= \max_{\omega \in \Omega_i^k} (\|\omega\|) \\ &= \max_{k^{-2}(\omega - \mu_i)^T \Sigma^{-1}(\omega - \mu_i) \leq 1} \left(\sqrt{\omega^T \omega} \right) \end{aligned} \quad (4.12)$$

which can be simplified with the change of variable $\phi = \omega - \mu_i$:

$$\gamma_i^k = \max_{k^{-2}\phi^T \Sigma^{-1} \phi \leq 1} \left(\sqrt{(\phi + \mu_i)^T (\phi + \mu_i)} \right) \quad (4.13)$$

After computing γ , the upper bound on the position uncertainty can be obtained in the same way as before ($\varepsilon = \gamma \cdot t_\varepsilon$). As a consequence of having a non-zero mean, computing the probability associated with the over-approximated disturbance and uncertainty sets is no longer straightforward to compute. Instead, we now have to integrate the probability density function (with the estimated parameters μ_i and γ_i) over $\Omega_{i(over)}^k$ to obtain that probability:

$$\begin{aligned} P[x(t_i) \in \Delta_i^k] &= P[x(t_i) \in \Omega_i^k] \\ &= \int_{\Omega_{i(over)}^k} f_\omega(\omega) \end{aligned}$$

In order to have good estimates, we need to have a certain amount of measurements, so these results need to be applied with care.

4.3 Application to the multi agent problem

Estimating the disturbance set in the multi-agent scenario isn't much more complex than in the single-agent scenario. Making use of the centralized structure described in the previous chapter, every agent k can, at each stopping instant t_i , report the measured average disturbance $\bar{\omega}_i^k$ to the leader, where the estimation procedure takes place. Here, we have the same recursive equations that we had in the previous scenario, with the difference that we obtain the i -th estimate by updating the previous estimate with the N new measurements, where N is the number of agents in the network. Note that for this approach to be valid, the disturbance set has to be approximately the same for the whole network - in other words, the spatial variation of the disturbances has to be such that it can be described by the same model for an area of the same size as the agent formation.

Chapter 5

Numerical Examples

Alongside with the theoretical study, a practical implementation was done in MATLAB, and some of the results obtained with the simulations made are shown in this chapter. In these, the disturbance set is constant and normally distributed (that is: $\Omega \sim (\mu, \Sigma)$), and we will focus on non-zero mean disturbance sets, as these are the cases where the difference between the two proposed control strategies become noticeable.

5.1 Single agent

In the following examples, we have that

- $x_{target} = [500, 500]^T$,
- $t_{target} = 140$,

Additionally, for the single-agent examples we set the upper bound on the position uncertainty, ε , to be equal to 20 meters. An important aspect of the following (single agent) simulations is that, to facilitate a comparative analysis, *in each example, the values of the external disturbance ω are kept the same for both control strategies.*

Example 1 Here we let $\mu = [-1, 1]$ and $\Sigma = 0.5^2 I$, where I denotes the 2×2 identity matrix. In a conservative solution, we can set γ considering $2^2 \Sigma$ ellipsoid, that is $\gamma = \|\mu\| + 2 \times 0.5 = \sqrt{2} + 1 \approx 2.414$. By setting γ this way, the over approximating set will include the Σ and $2^2 \Sigma$ ellipsoids, so the probability of the agent stopping within ε meters of the waypoint will always be greater than 86% (see figure 5.1(a)).

For simulation purposes, however, we set $\gamma = 2.5$. Thus,

$$\begin{aligned} t_\varepsilon &= \frac{\varepsilon}{\gamma} \\ &= \frac{20}{2.5} \\ &= 8 \text{ seconds} \end{aligned}$$

and

$$\begin{aligned} N &= \left\lfloor \frac{t_{\text{target}} - t_0}{t_\varepsilon} \right\rfloor \\ &= \left\lfloor \frac{140 - 0}{8} \right\rfloor \\ &= \lfloor 17.5 \rfloor \\ &= 17 \text{ waypoints} \end{aligned}$$

t_f is then equal to $140 - 17 \times 8 = 4$ seconds.

Example 2 In this example we set γ in a less conservative way, without taking the mean into consideration: $\gamma = 2 \times 0.5 = 1$. This way, unlike what happened in the previous example, the over-approximating set will not (even) include the Σ ellipsoid, and the probability of the agent stopping within ε meters of the waypoint will be greatly reduced.

We have

$$\begin{aligned} t_\varepsilon &= \frac{\varepsilon}{\gamma} \\ &= \frac{20}{1} \\ &= 20 \text{ seconds} \end{aligned}$$

and

$$\begin{aligned} N &= \left\lfloor \frac{t_{\text{target}} - t_0}{t_\varepsilon} \right\rfloor \\ &= \left\lfloor \frac{140 - 0}{20} \right\rfloor \\ &= \lfloor 7 \rfloor \\ &= 7 \text{ waypoints} \end{aligned}$$

t_f is then equal to $140 - 20 \times 7 = 0$ seconds (no final approach).

5.1.1 Trajectory

In figures 5.2 and 5.3, the estimated and true trajectories are shown in blue and red (respectively), with the blue circles representing the set of positions within ε meters of the corresponding waypoint. If our choice of γ is appropriate, then the stopping positions (black dots) will always lie inside these discs.

Comparing figures 5.2(a) and 5.2(b), we see how each of the two control strategies responds to the non-zero mean scenario. $h_1(\cdot)$ shows a greater "sensitivity" to the mean disturbance when compared to $h_2(\cdot)$, as we see that for the former there is a distortion of the trajectory (when compared to the straight-line ideal trajectory) in the direction of the mean disturbance. There is also a difference in the respective control signal norms (figures 5.2(e) and 5.2(f)) due to a fact that we have already mentioned - $h_1(\cdot)$ takes longer to compensate for a position drift than $h_2(\cdot)$, something that becomes very noticeable when, as in this case, the average position drift is not close to zero. Finally, for both scenarios, we can see a smaller circle in the figures depicting the final approach part of the trajectory (figures 5.2(c) and 5.2(d)). This circle has a radius of $\gamma \cdot t_f = 2.5 \times 4 = 10$ meters, as defined by equation 2.46.

Notice that for almost all waypoints, the agents stops inside the circle of radius ε (drawn in blue), so our choice for γ although conservative, yielded good results. The same can't be said for the next example, where a (very) relaxed choice of γ resulted in the agent failing to stop within ε meters of the waypoint at almost all instants. The success (or failure) of the agent in stopping inside the discs of radius ε is a direct consequence of the choice of γ - even though for a normally distributed set is impossible to choose γ in such a way that the upper bound on the position uncertainty will *always* hold, a low value will result in the agent failing to be inside the disc most of the times as, consequently, the probability of $\omega_{in\Omega_{over}}$ will be very low. On the other hand, a very high value of γ will result in an over-approximating set Ω_{over} that will most likely contain some of the disturbance set's confidence ellipsoids, and thus the upper bound will hold very often. The choices of γ for the two examples above are shown in figure 5.1.

In what concerns the trajectories, the difference isn't as accentuated as in the previous example, mainly because of the larger time intervals - since t_ε for example 2 is more than double than that for example 1 with the disturbance set remaining the same, the vehicle will drift further away. Consequently, the difference in the control signal norms is much smaller. Also, notice that due to our choice of γ there is no time left for the final approach and the agent stops, using either control strategy, at more than ε meters from the target.

5.1.2 Disturbance Set Estimation

In figure 5.4, the $\mathcal{E}(\mu, k^2\Sigma)$ ellipsoids of the true disturbance set are shown in blue, while the corresponding estimated ellipsoids at the end of the trajectory, $\mathcal{E}(\mu_N, k^2\Sigma_N)$ are shown in red. In

the remaining the estimation errors at each stopping instant t_i are plotted. The estimation error of the covariance is at the instant t_k defined as

$$e_k^\Sigma = \sigma_1(\Sigma - \Sigma_k)$$

where $\sigma_i(A)$ denotes the i -th largest singular value of the A matrix, and the estimation error of the mean as

$$e_k^\mu = \|\mu - \mu_k\|$$

Looking at figures 5.4(a) and 5.4(b) we immediately see the difference between the disturbance set estimates - even though neither is a very good estimate, the one obtained using 17 measurements is, as we would expect, much better than the one obtained using less than half ($N = 7$) measurements. Still, these numbers are too low (and too close) to draw significant conclusions regarding the convergence of the estimation errors.

5.2 Multi agent

In the multi-agent examples, we will use the network depicted in figure 5.5 with a *range* parameter of 90 meters. For the network graph in figure 5.5, we have

$$\begin{aligned} G &= \{N, E\} \\ N &= \{a_1, a_2, a_3, a_4, a_5\} \\ E &= \{\{a_1, a_2\}, \{a_1, a_3\}, \{a_2, a_4\}, \{a_3, a_5\}\} \end{aligned}$$

with

$$A = \begin{bmatrix} 0 & 1 & 1 & 0 & 0 \\ 1 & 0 & 0 & 1 & 0 \\ 1 & 0 & 0 & 0 & 1 \\ 0 & 1 & 0 & 0 & 0 \\ 0 & 0 & 1 & 0 & 0 \end{bmatrix} \quad D = \begin{bmatrix} 2 & 0 & 0 & 0 & 0 \\ 0 & 2 & 0 & 0 & 0 \\ 0 & 0 & 2 & 0 & 0 \\ 0 & 0 & 0 & 1 & 0 \\ 0 & 0 & 0 & 0 & 1 \end{bmatrix}$$

and

$$L = \begin{bmatrix} 2 & -1 & -1 & 0 & 0 \\ -1 & 2 & 0 & -1 & 0 \\ -1 & 0 & 2 & 0 & -1 \\ 0 & -1 & 0 & 1 & 0 \\ 0 & 0 & -1 & 0 & 1 \end{bmatrix}.$$

Recalling the results we derived in the multi-agent chapter we know that ε has to be such that (equation 3.18)

$$\varepsilon < \frac{1}{2} \min(d_{i,j}), \text{ with } i \neq j$$

holds, in order to prevent collisions. Since the smallest inter-agent distance in the network is equal to $50\sqrt{2}$, we have that

$$\varepsilon < 25\sqrt{2}$$

We also know that to keep the network connected, equation 3.19 must also hold

$$\varepsilon \leq \min_{i \in A} \left[\frac{1}{2} \left(r - \max_{j \in \mathcal{N}(i)} (d_{i,j}) \right) \right]$$

Looking at figure 5.5(b), we see that the largest inter-agent distance between any two directly connected agents is also equal to $50\sqrt{2}$ meters. This yields

$$\varepsilon \leq 9.65$$

which is a seemingly conservative value, a consequence of wanting to maintain the network graph unchanged at every stopping instant. Still, in the first two examples we will use $\varepsilon = 10$ meters.

We will set the target to be located at $x_{target} = [500, 0]^T$, with $t_{target} = 100$ seconds, and let the disturbance set be the same as in the single agent examples, that is, $\mu = [-1, 1]$ and $\Sigma = 0.5^2 I$. Finally, just as we did for the single agent examples, to facilitate a comparative analysis, *in each example, the values of the external disturbance ω are kept the same for both control strategies.*

Example 3 *In this first example we choose γ in the same way as we did in the first example, that is, the norm of the mean disturbance plus 2σ : $\gamma = \sqrt{2} + 2 \times 0.5 \approx 2.414$. And, just as we did in that example, we set $\gamma = 2.5$. This way we have*

$$\begin{aligned} t_\varepsilon &= \frac{\varepsilon}{\gamma} \\ &= \frac{10}{2.5} \\ &= 4 \text{ seconds} \end{aligned}$$

and

$$\begin{aligned}
 N &= \left\lfloor \frac{t_{\text{target}} - t_0}{t_\varepsilon} \right\rfloor \\
 &= \left\lfloor \frac{100 - 0}{4} \right\rfloor \\
 &= \lfloor 25 \rfloor \\
 &= 25 \text{ waypoints}
 \end{aligned}$$

t_f is then equal to $100 - 25 \times 4 = 0$ seconds (no final approach).

Example 4 In this example we set γ as 3σ , that is, 1.5. The reason we do not take the mean disturbance is that it is the same for all the agents in the network and thus, by itself, it is not capable of affecting connectivity or of causing collisions between any two agents. As such, we are only concerned with the covariance, and we use it to define γ .

$$\begin{aligned}
 t_\varepsilon &= \frac{\varepsilon}{\gamma} \\
 &= \frac{10}{1.5} \\
 &= \frac{20}{3} \\
 &= 6.(6) \text{ seconds}
 \end{aligned}$$

and

$$\begin{aligned}
 N &= \left\lfloor \frac{t_{\text{target}} - t_0}{t_\varepsilon} \right\rfloor \\
 &= \left\lfloor \frac{100 - 0}{6.(6)} \right\rfloor \\
 &= \lfloor 15 \rfloor \\
 &= 15 \text{ waypoints}
 \end{aligned}$$

t_f is then equal to $100 - 15 \times 6.(6) = 0$ seconds (no final approach).

Example 5 In this final example, we illustrate the importance of the choice of ε in multi-agent applications, by doubling its value, that is, $\varepsilon = 20$ meters, and keeping the remaining parameters the same as they were in the previous example.

5.2.1 Trajectory

Most of the conclusions that we are able to draw from examples 3 and 4 are very similar to those drawn in the single agent scenario, namely, the greater sensitivity to disturbances of the $h_1(\cdot)$ control strategy when compared to $h_2(\cdot)$ (as can be seen in figures 5.6/5.8 and 5.10/ 5.12) and the influence of the choice of γ on our result on the upper bound on the position uncertainty.

There are, however, some interesting results due to the leader's use of the different control strategies. Take, for example, the agents' control signal norms in example 3, figure 5.7. Here, we see not only an increasing $\|u\|$, typical of this control strategy when under an adverse average disturbance, but also a greater variation in the followers' speeds when compared to that of the leader - something which is easily understandable as we know, from equation 3.5, that each follower not only has to compensate for its own drift, but also for the leader's. Here, we see that the $h_2(\cdot)$ control strategy outperforms $h_1(\cdot)$ (figure 5.9), as not only $\|u\|$ is no longer increasing, and the variations in the followers' speeds are of the same magnitude as that of the leader. The justification is the same as before, but given the way that the leader sets its speed, the follower only needs to compensate for its own drift (see equation 3.8). These conclusions are also valid for example 4, as we can see from figures 5.11 and 5.11.

5.2.2 Connectivity

In the plots of the formation trajectory of examples 3 to 5, we are able to see black, dashed lines indicating the presence of a direct connection between two agents - this way we're able to see how the network graph evolves along the trajectory. While in the first two multi-agent examples the graph remains the same, in the third example there is a loss of connectivity and agents a_3 and a_5 are lost. Since the difference between the second and third examples is just the choice of ε , we are able to say that albeit conservative, the range and collision conditions stated in the end of chapter 3, are very useful to the choice of an adequate ε . Still, the choice of ε alone is not enough since, the simplification used in examples 4 and 5 notwithstanding, a poor choice of the value of γ will annul the result on the upper bound on the position uncertainty and the reasoning used to obtain the said conditions will no longer be valid.

5.2.3 Disturbance Set Estimation

Finally, in figure 5.14 the advantage of performing estimation using more than one agent becomes evident, as instead of just 1, there are now 5 new measurements at each waypoint. And despite the smaller number of waypoints in example 4 when compared to example 4, which results in a difference of $(5 \times 26) - (5 \times 15) = 55$ measurements, both the estimated sets and the associated

estimation errors are very similar and, as it should be expected, show a considerable improvement compared to the single agent examples.

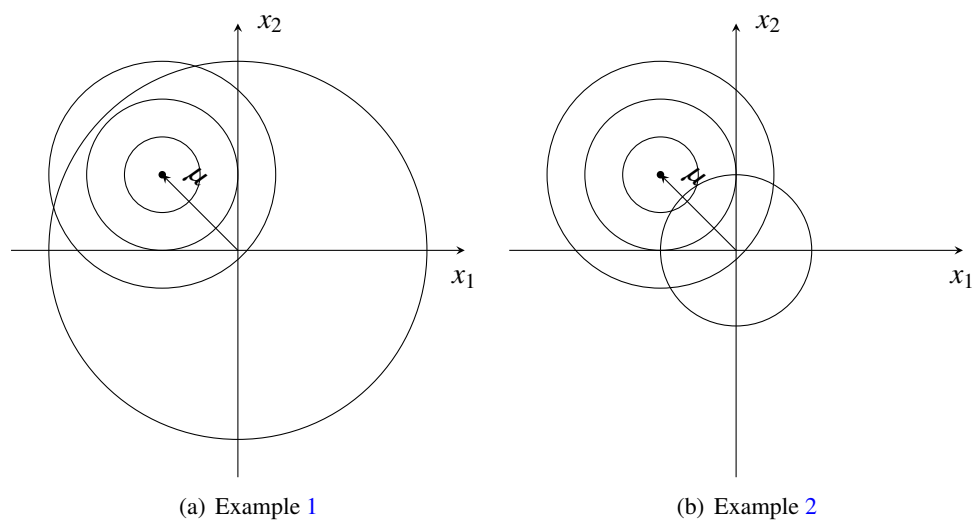
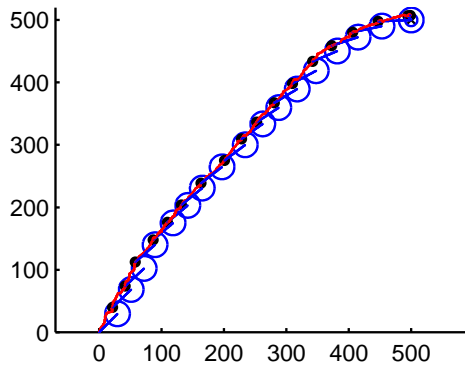
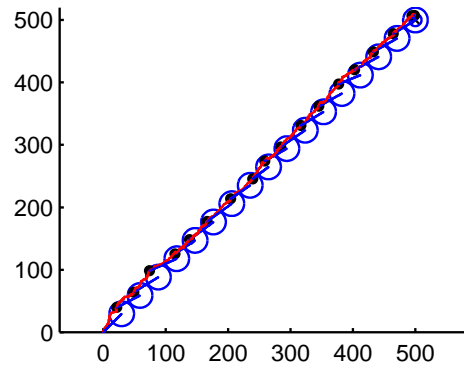


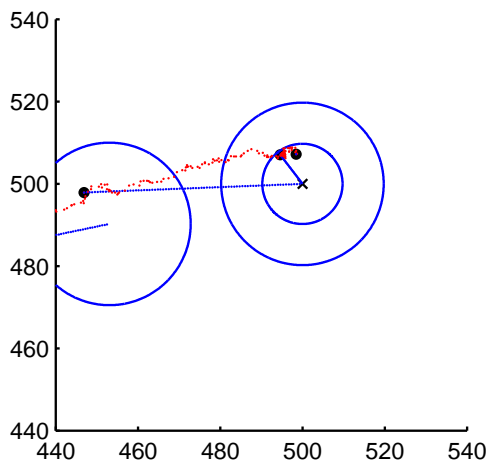
Figure 5.1: The disturbance set's confidence ellipsoids $\mathcal{E}(\mu, k^2 \Sigma)$ for $k = \{1, 2, 3\}$ and the over-approximating disturbance set for examples 1 (left) and 2 (right).



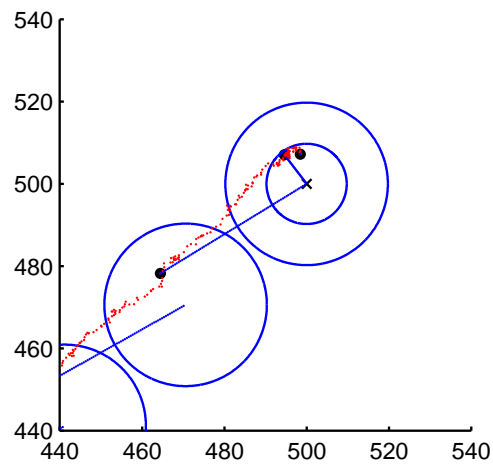
(a) Trajectory for the $h_1(\cdot)$ control strategy



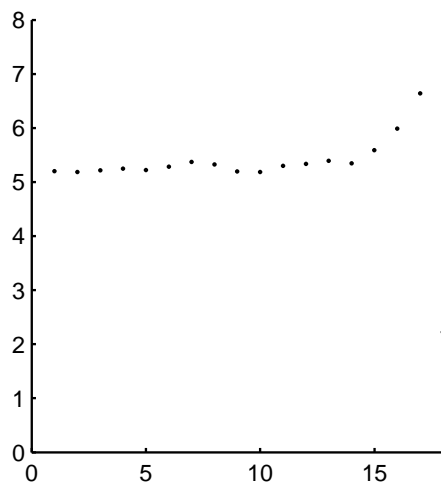
(b) Trajectory for the $h_2(\cdot)$ control strategy



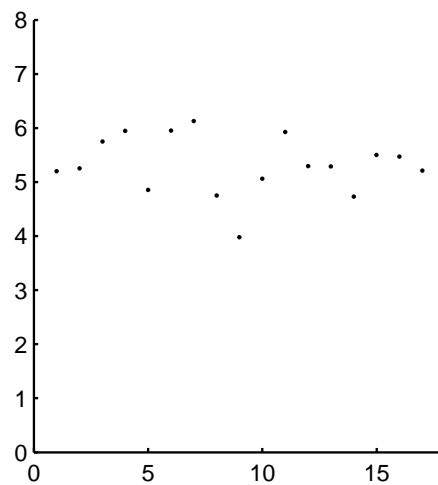
(c) Final approach part of the trajectory ($h_1(\cdot)$)



(d) Final approach part of the trajectory ($h_2(\cdot)$)

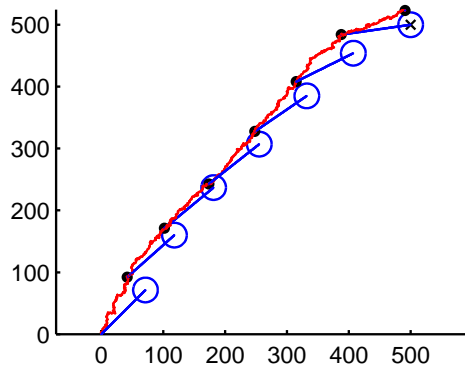


(e) Control signal norm for the $h_1(\cdot)$ control strategy

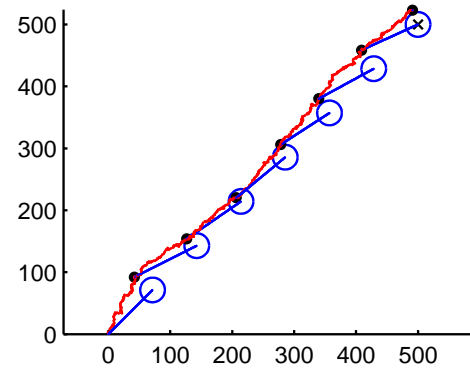


(f) Control signal norm for the $h_2(\cdot)$ control strategy

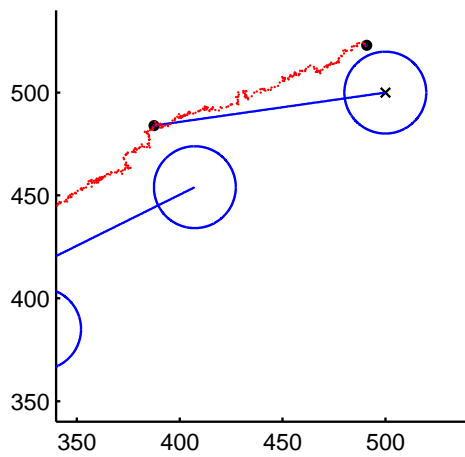
Figure 5.2: Example 1



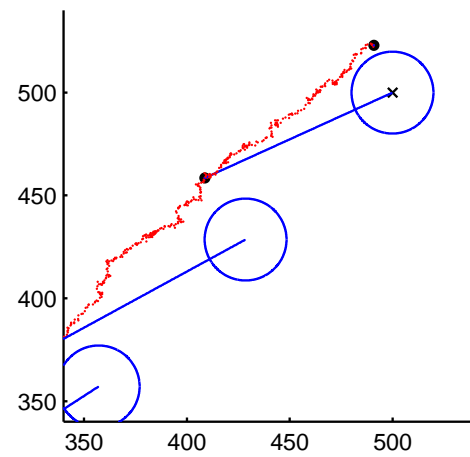
(a) Trajectory for the $h_1(\cdot)$ control strategy



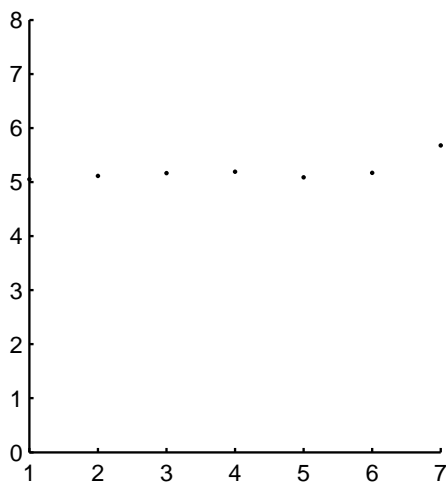
(b) Trajectory for the $h_2(\cdot)$ control strategy



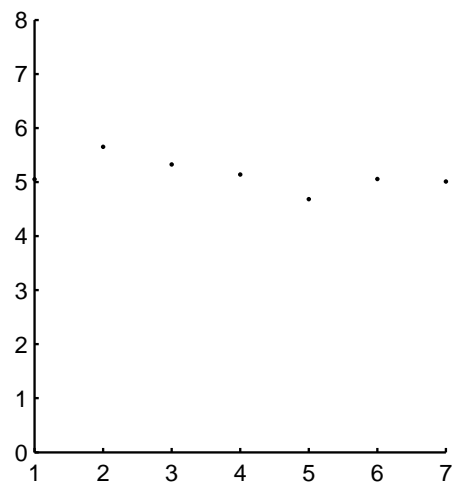
(c) Final approach part of the trajectory ($h_1(\cdot)$)



(d) Final approach part of the trajectory ($h_2(\cdot)$)

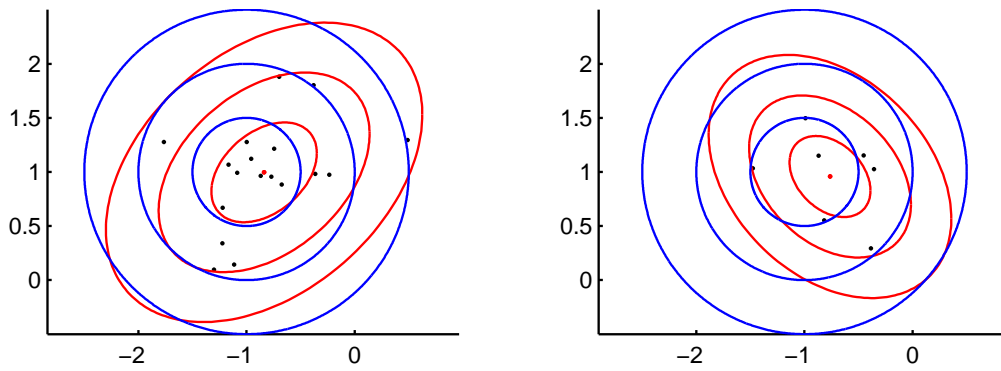


(e) Control signal norm for the $h_1(\cdot)$ control strategy

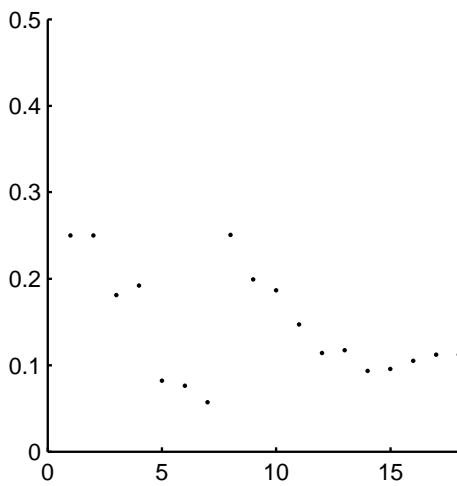


(f) Control signal norm for the $h_2(\cdot)$ control strategy

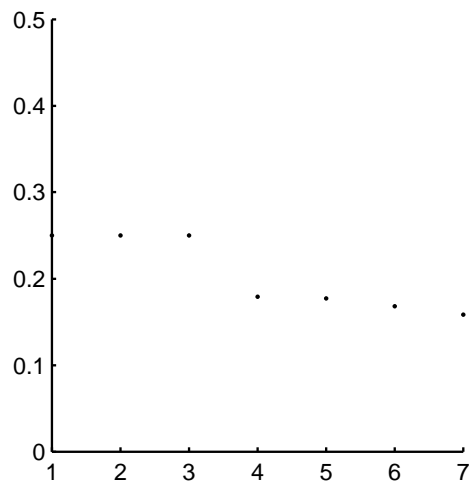
Figure 5.3: Example 2



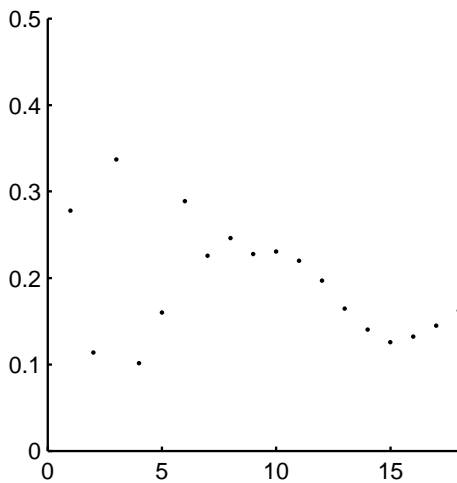
(a) Disturbance set estimate at the end of the trajectory for example 1 (b) Disturbance set estimate at the end of the trajectory for example 2



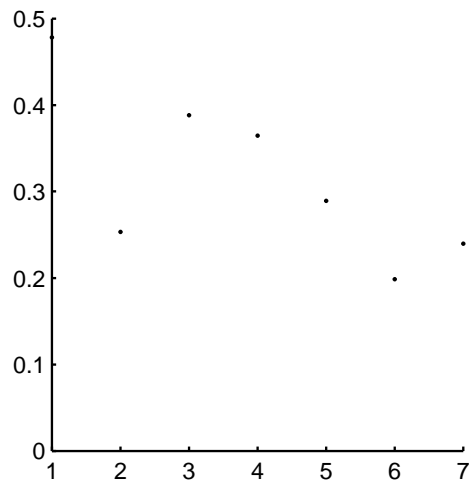
(c) Covariance estimation error for example 1



(d) Covariance estimation error for example 2



(e) Mean estimation error for example 1



(f) Mean estimation error for example 2

Figure 5.4: Disturbance set estimation in Examples 1 (left) and 2 (right)

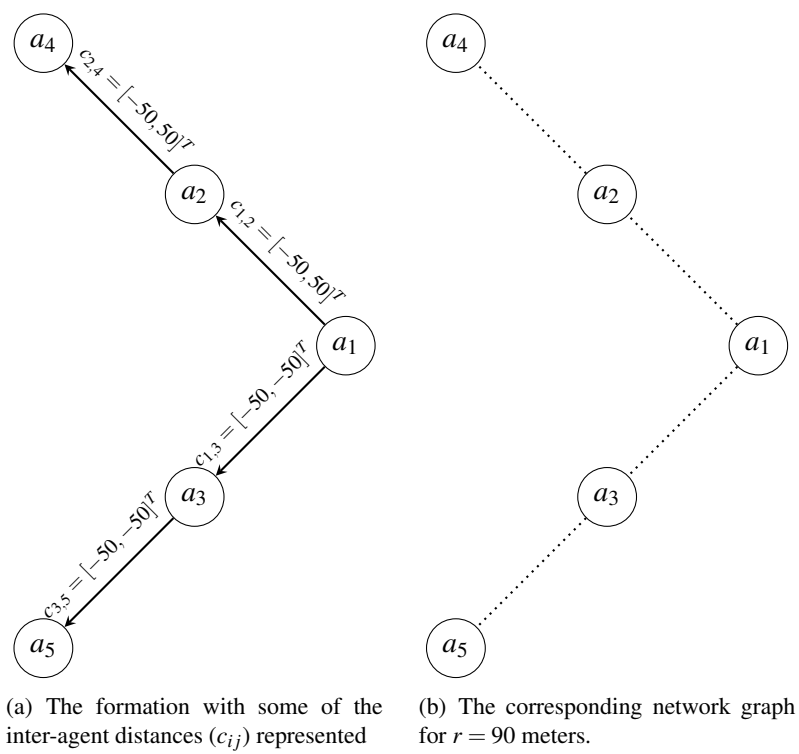


Figure 5.5: Example of a formation

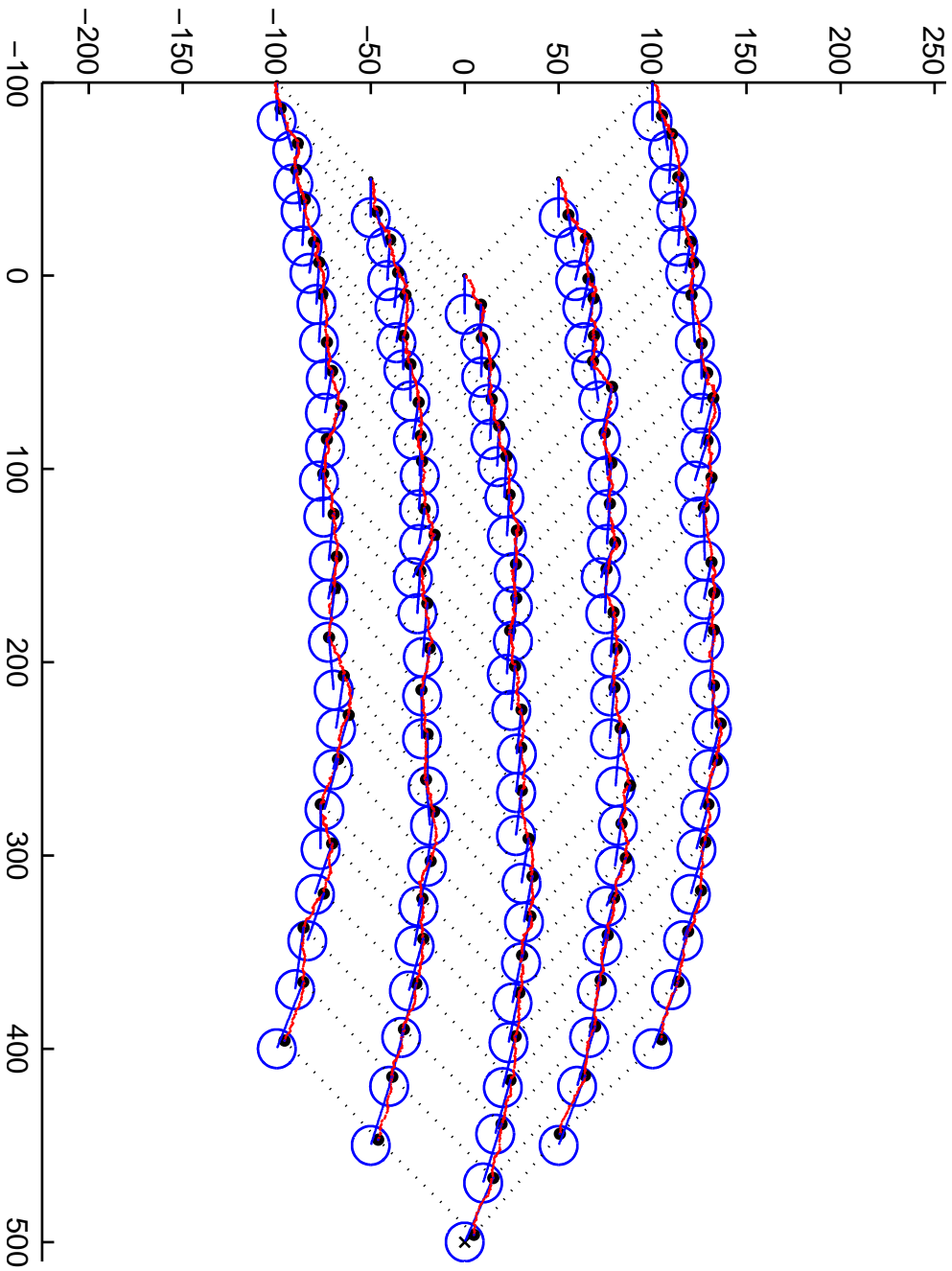
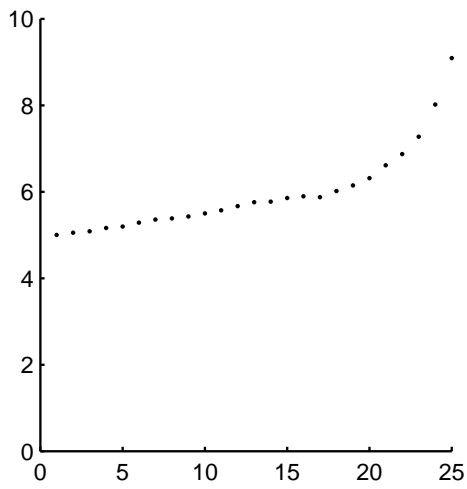
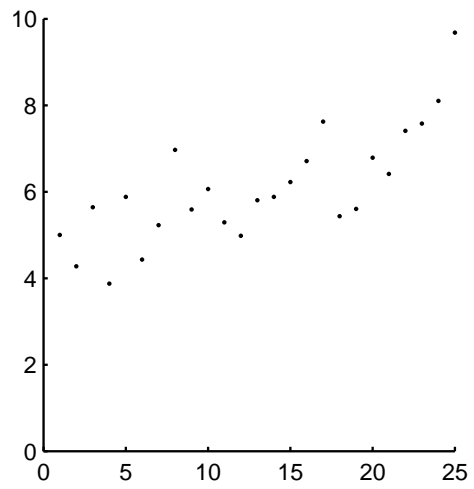


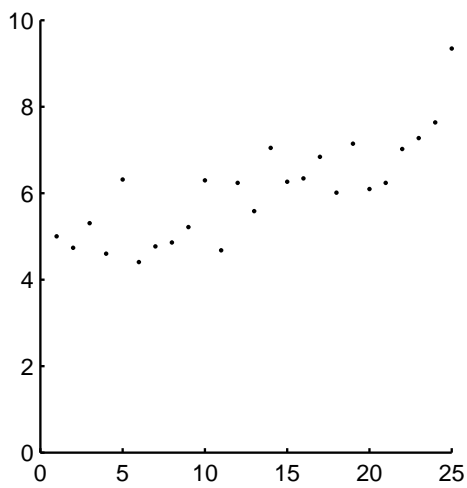
Figure 5.6: (Example 3) Formation trajectory using the $h_1(\cdot)$ control strategy



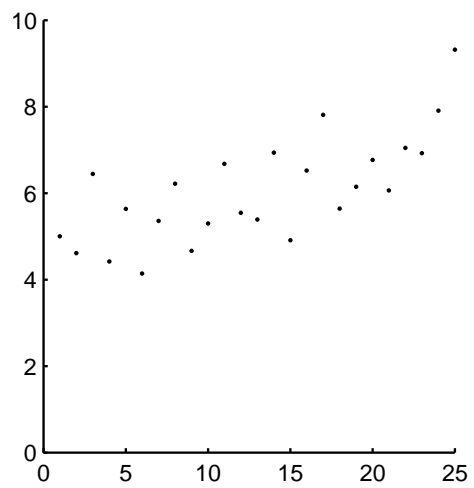
(a) a_1



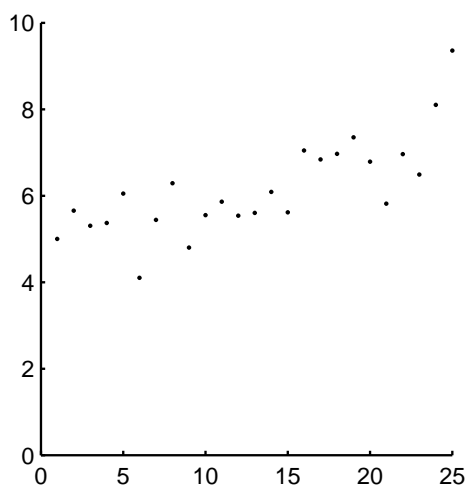
(b) a_2



(c) a_3



(d) a_4



(e) a_5

Figure 5.7: (Example 3) Control signal norms for the agents in the network using the $h_1(\cdot)$ control strategy

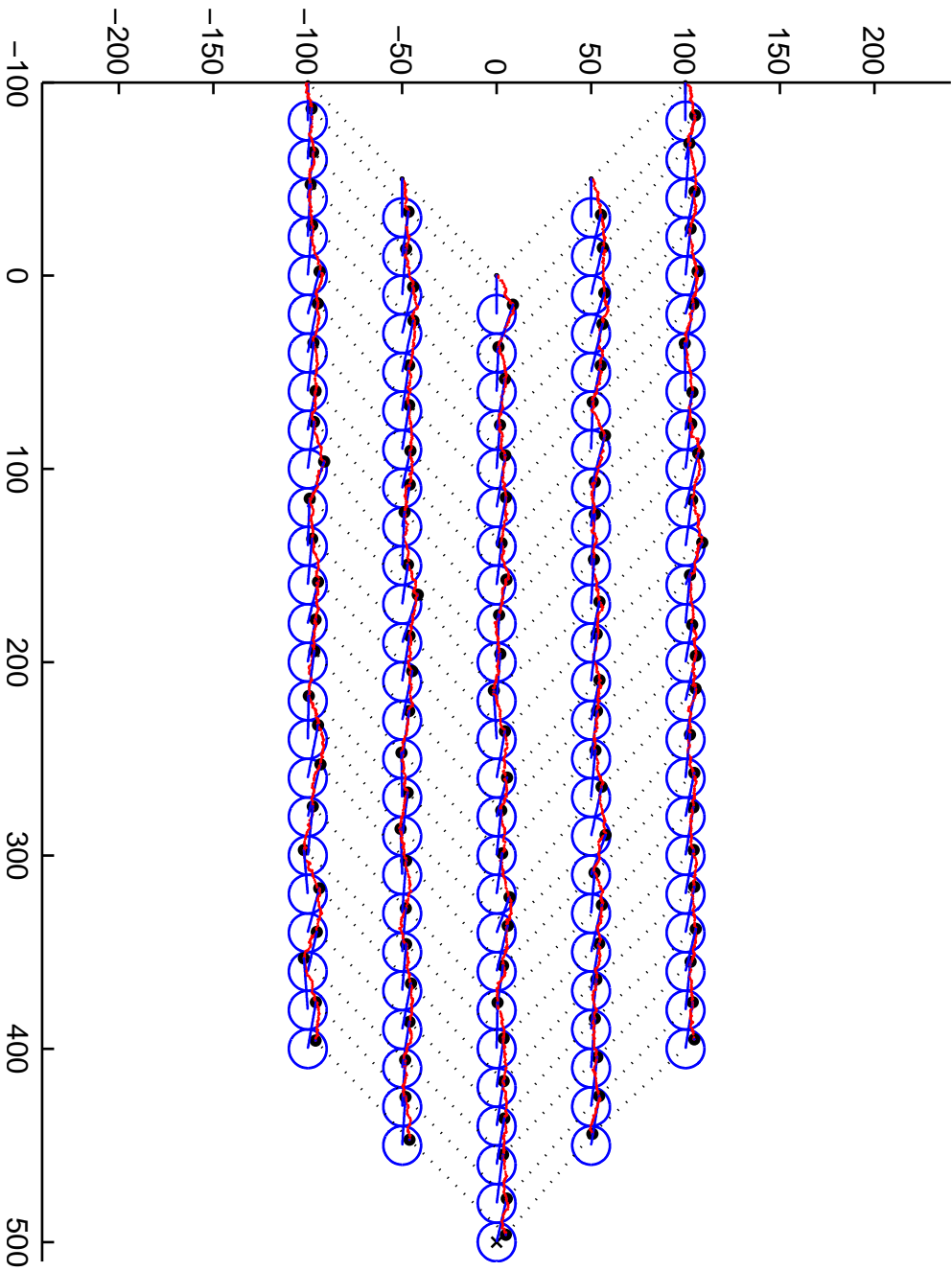


Figure 5.8: (Example 3) Formation trajectory using the $h_2(\cdot)$ control strategy

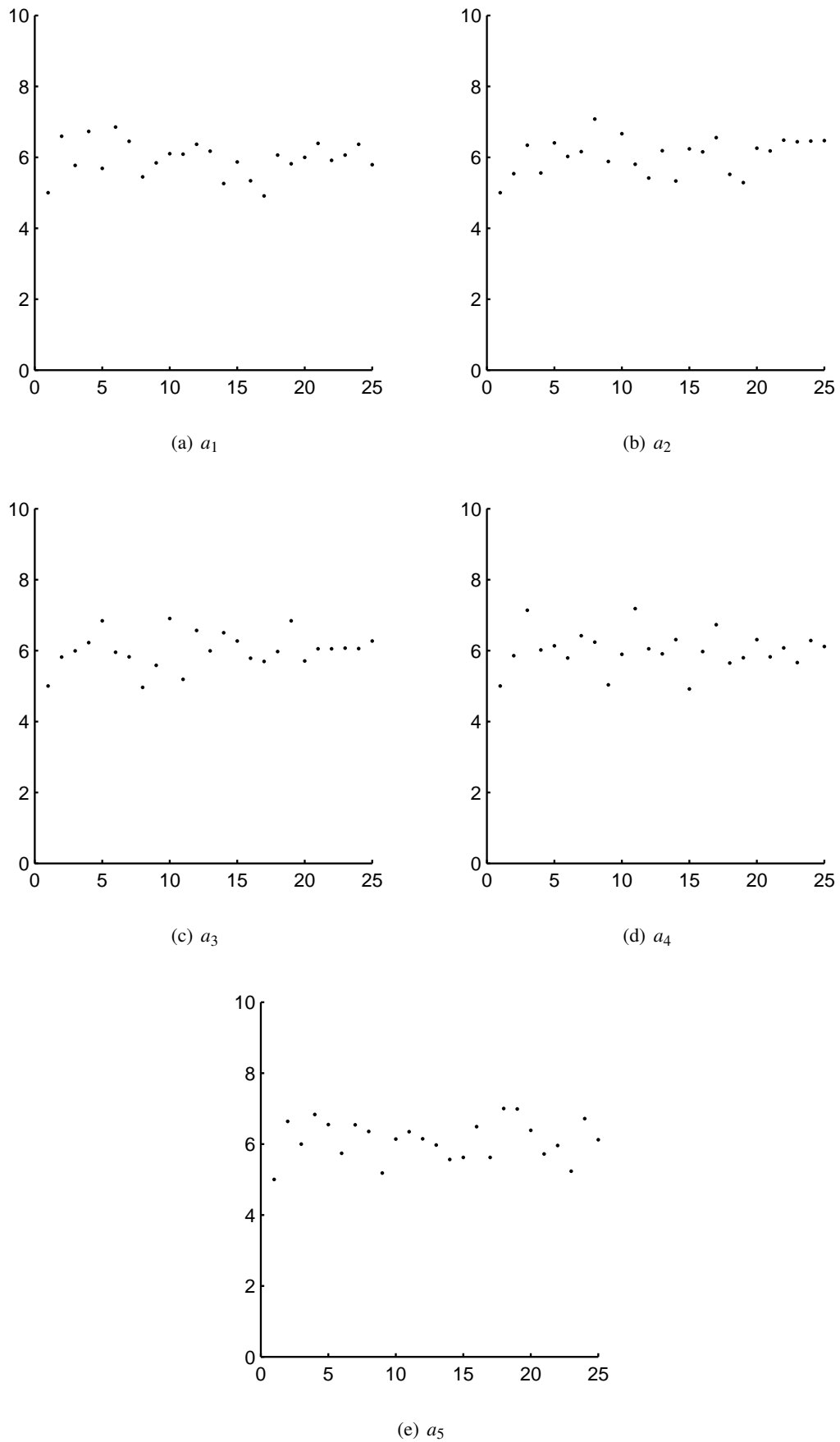


Figure 5.9: (Example 3) Control signal norms for the agents in the network using the $h_2(\cdot)$ control strategy

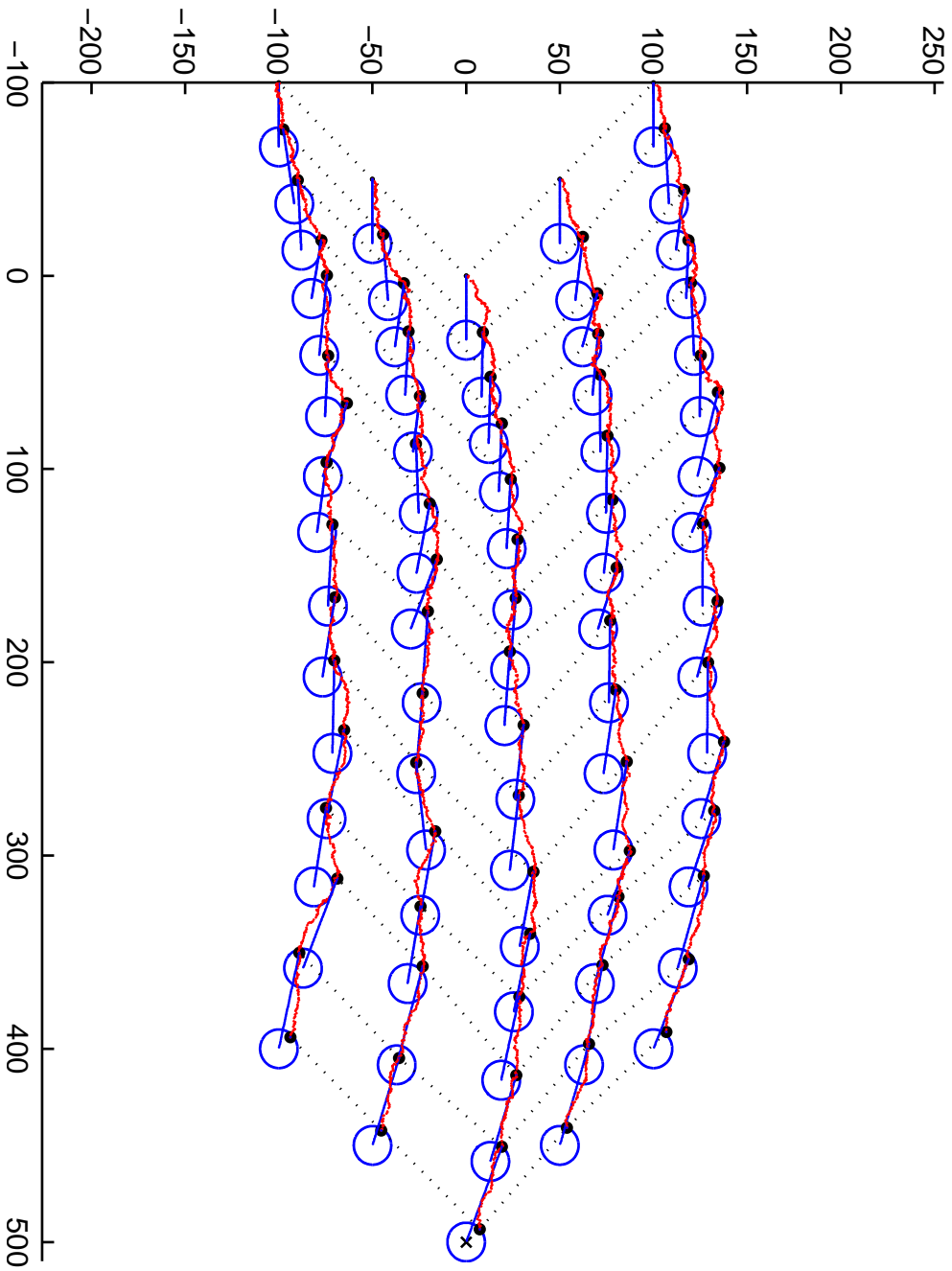


Figure 5.10: (Example 3) Formation trajectory using the $h_1(\cdot)$ control strategy

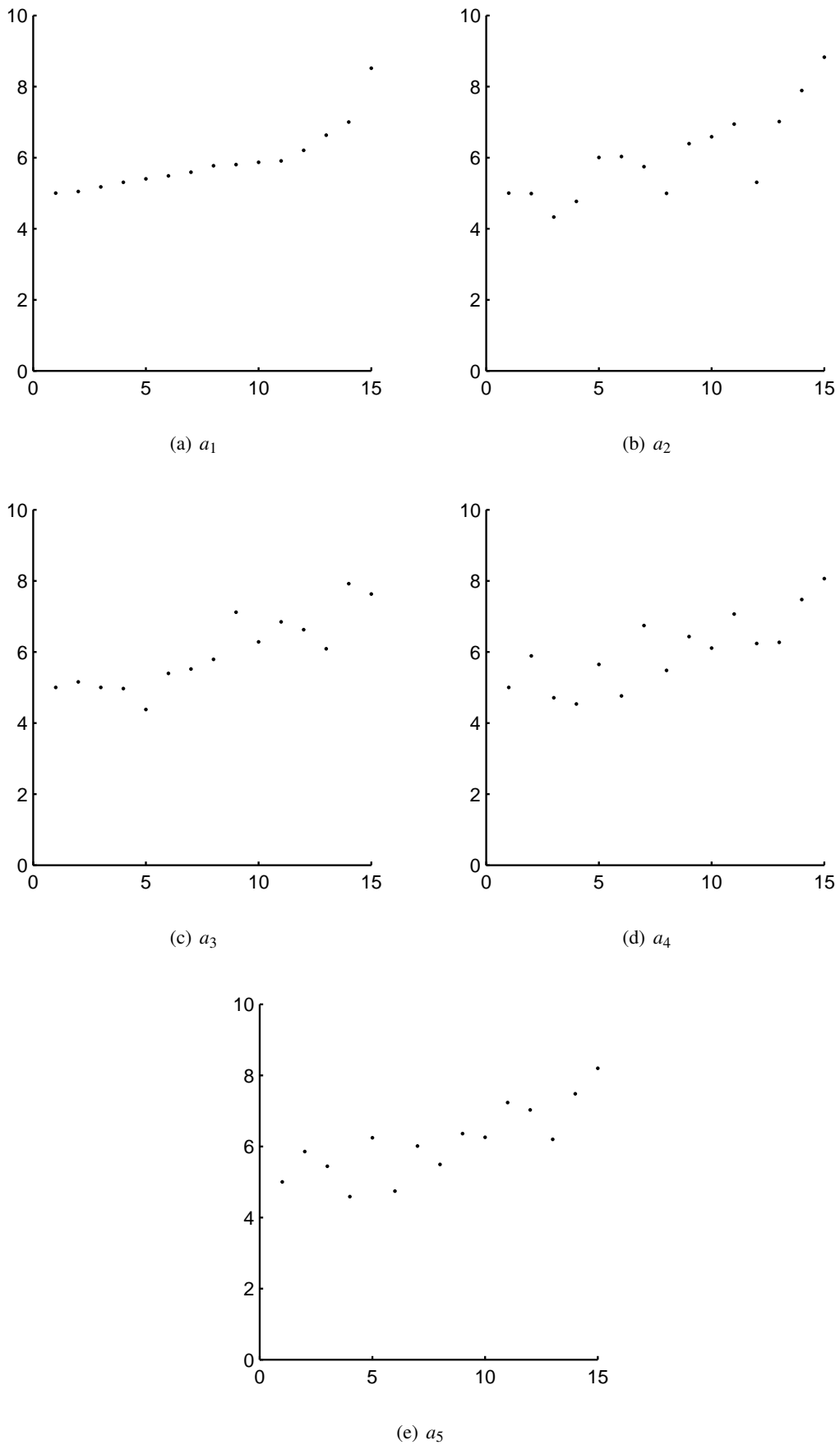


Figure 5.11: (Example 4) Control signal norms for the agents in the network using the $h_1(\cdot)$ control strategy

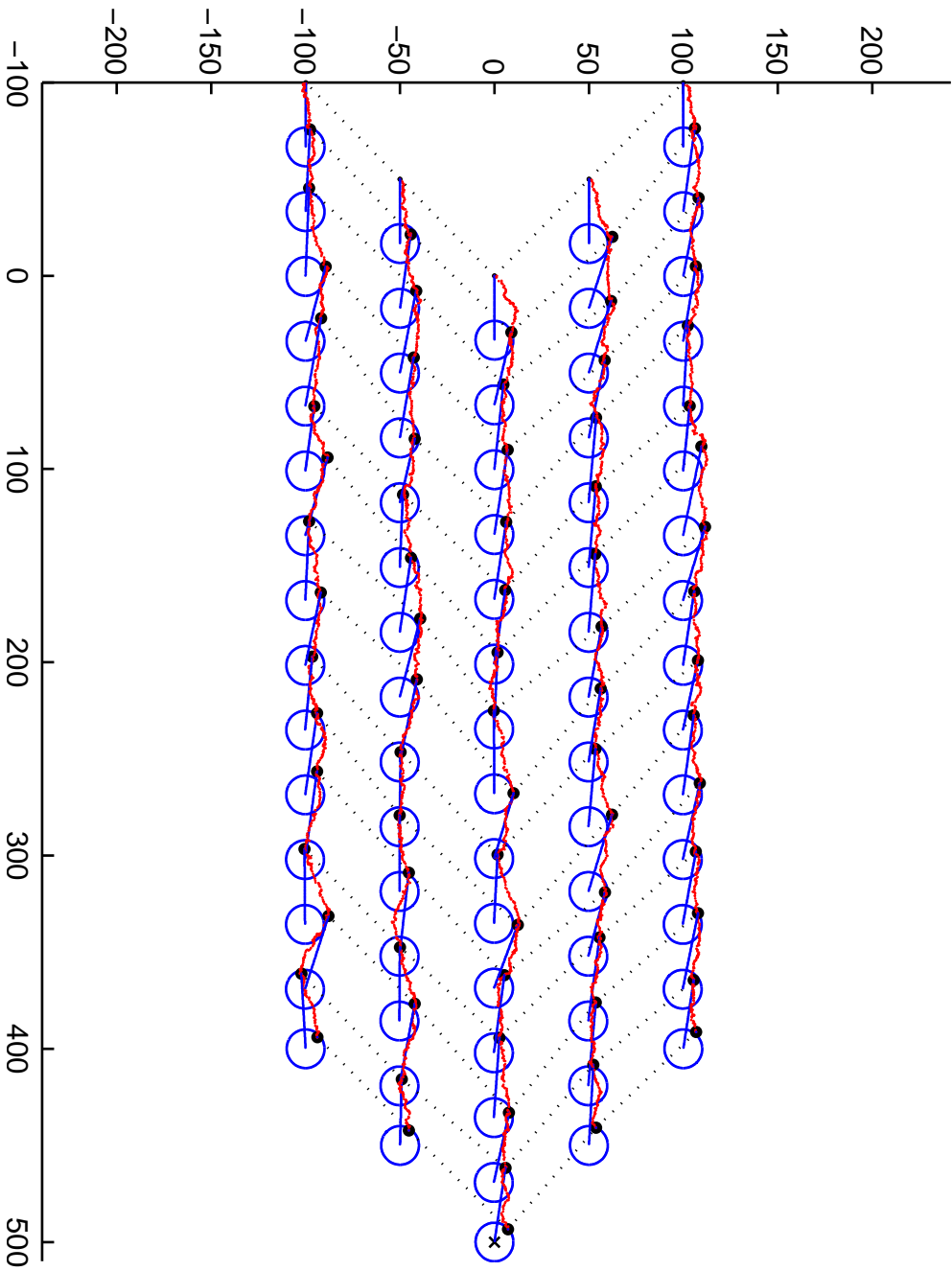


Figure 5.12: (Example 4) Formation trajectory using the $h_2(\cdot)$ control strategy

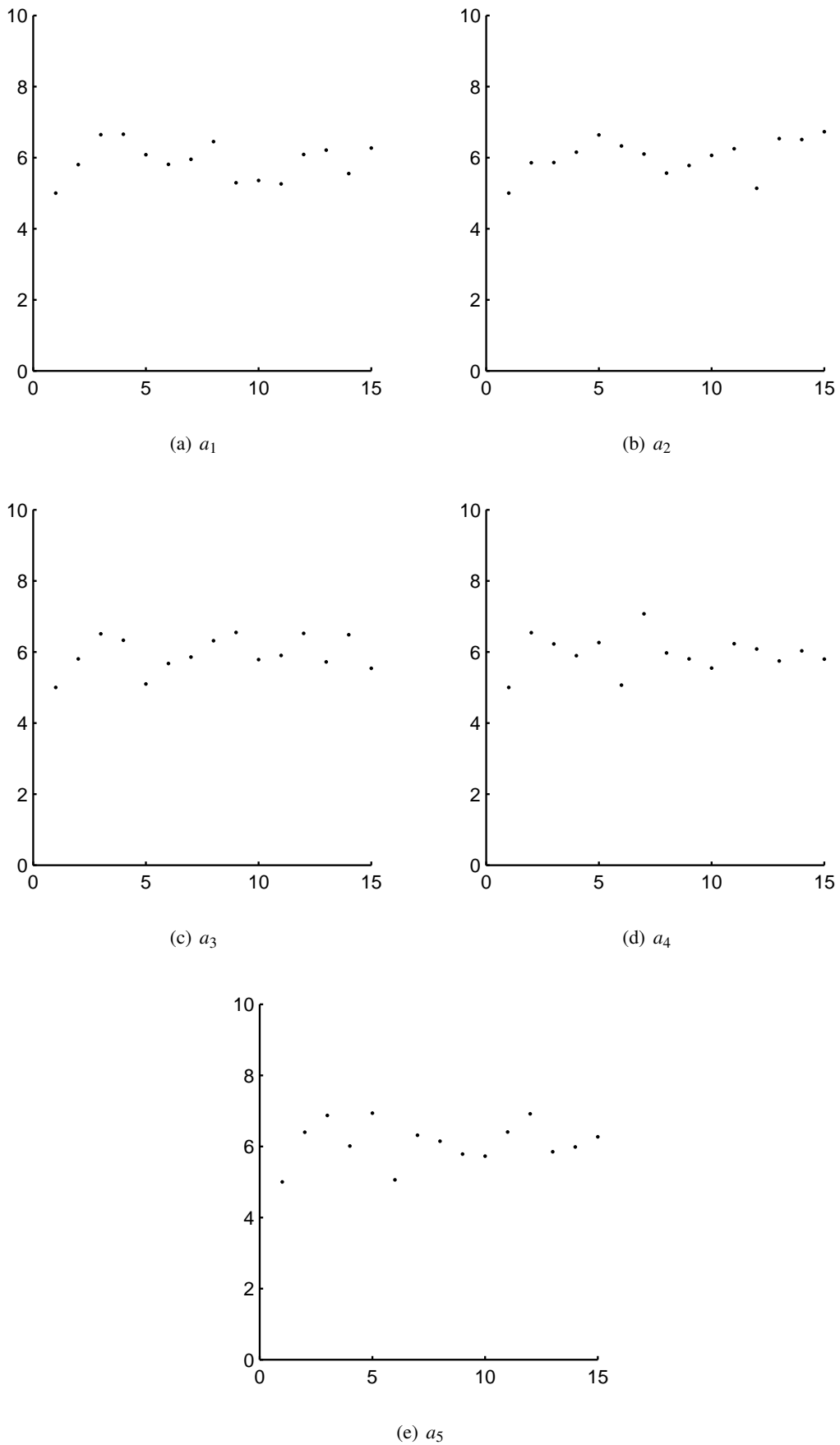
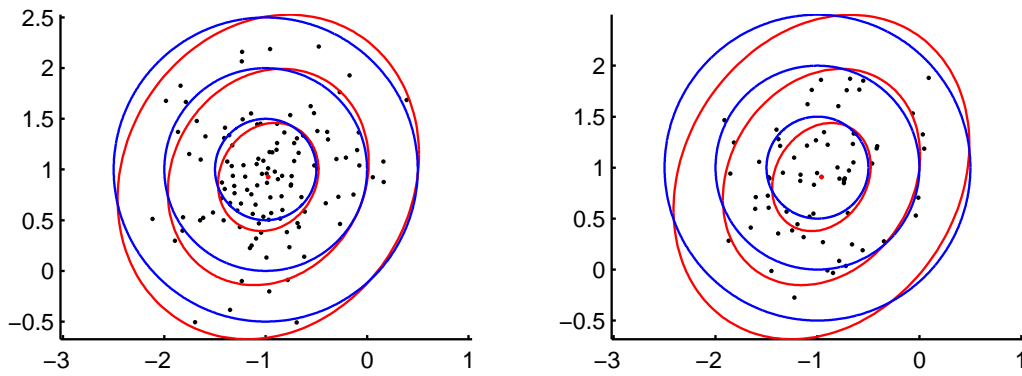
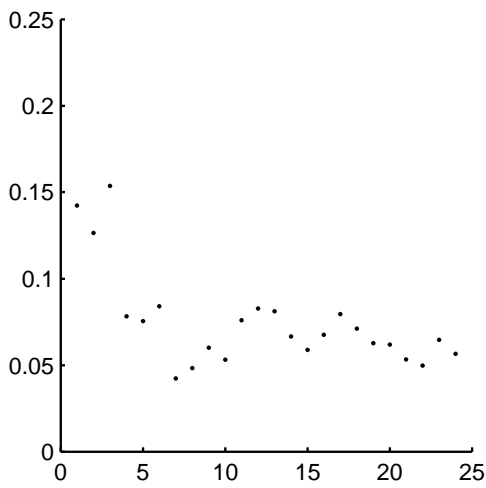


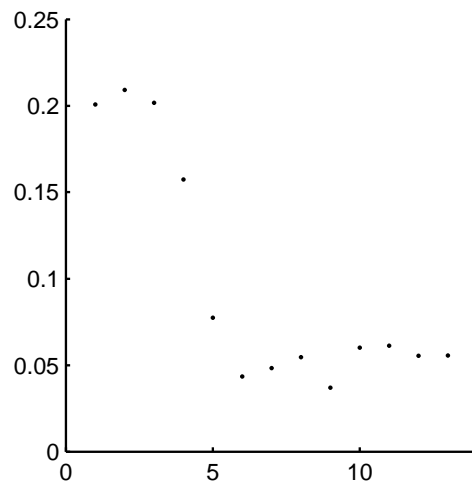
Figure 5.13: (Example 4) Control signal norms for the agents in the network using the $h_2(\cdot)$ control strategy



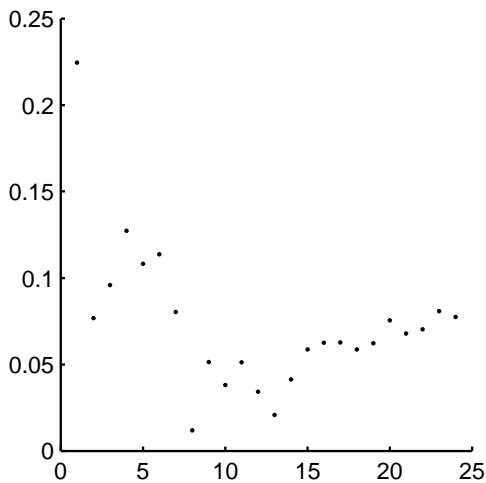
(a) Disturbance set estimate at the end of the trajectory for example 3 (b) Disturbance set estimate at the end of the trajectory for example 4



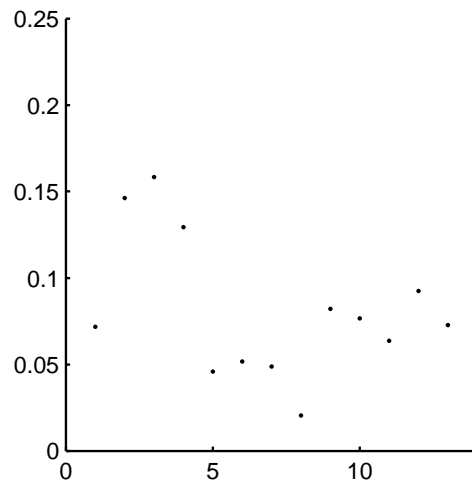
(c) Covariance estimation error for example 3



(d) Covariance estimation error for example 4



(e) Mean estimation error for example 3



(f) Mean estimation error for example 4

Figure 5.14: Disturbance set estimation in Examples 3 (left) and 4 (right)

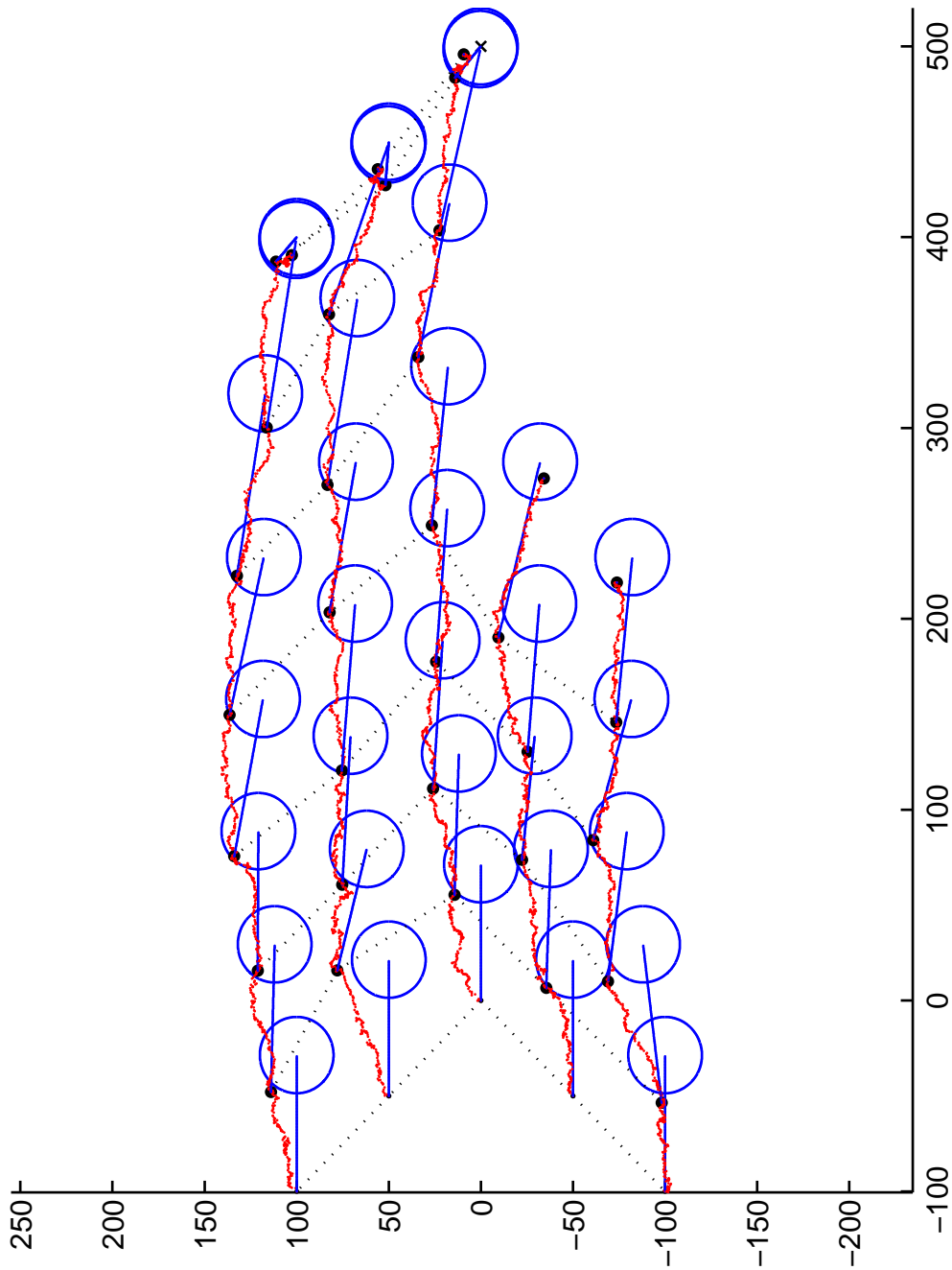


Figure 5.15: (Example 5) Formation trajectory using the $h_1(\cdot)$ control strategy

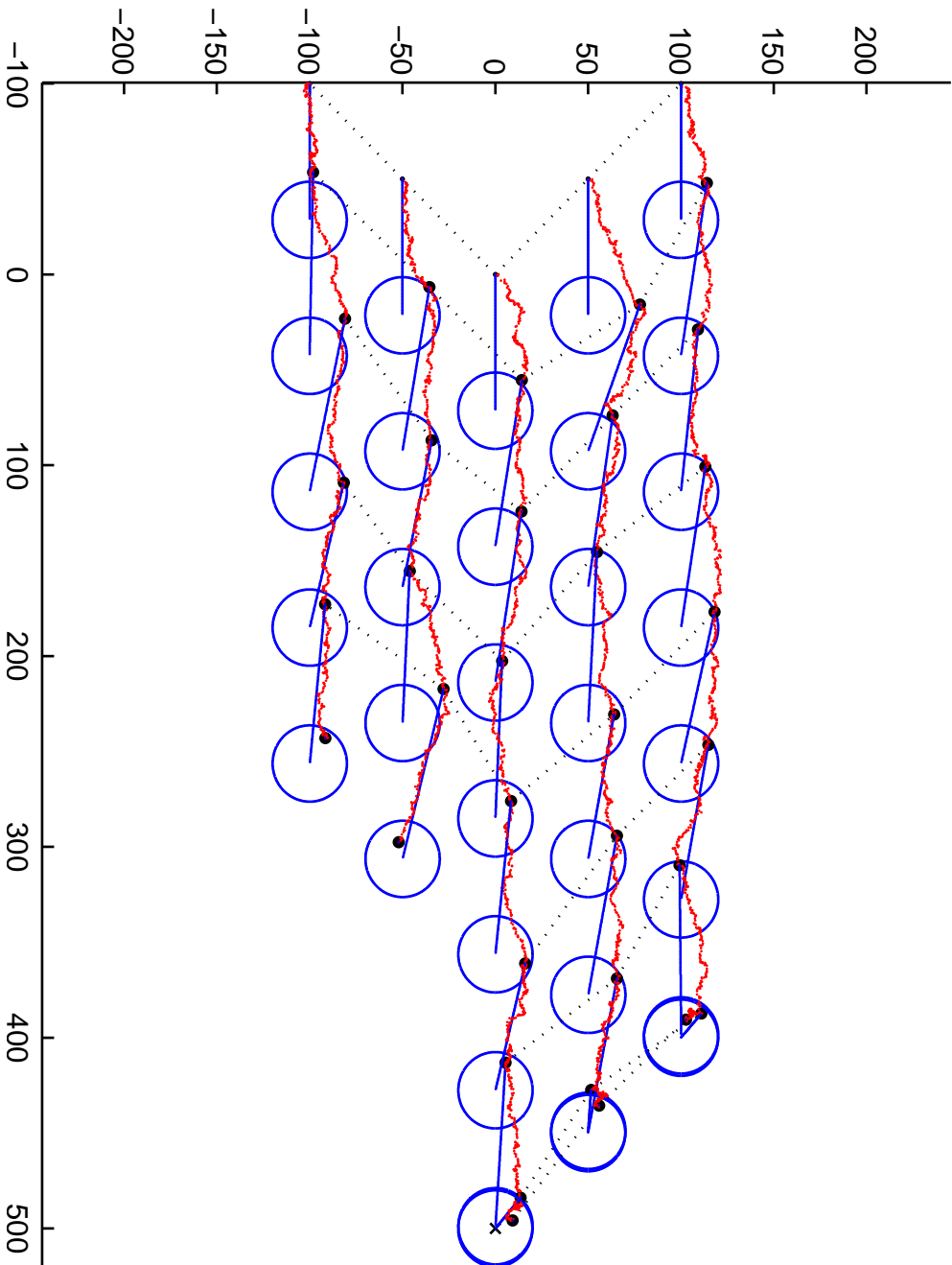


Figure 5.16: (Example 4) Formation trajectory using the $h_2(\cdot)$ control strategy

Chapter 6

Conclusions and Future Work

We have proposed a waypoint based approach to solve the multi-agent problem under communication and measurement constraints, which relies on a simplifying assumption on the disturbance set allowing us to have an upper bound on the position uncertainty growth rate - γ . This, together with the user-defined maximum position uncertainty ε is used to determine when the agent should stop. Two alternative control strategies are able to drive the agent to the target while guaranteeing that the agent's distance to its ideal position is never greater than ε . All of these results were derived for the single agent problem and later extended to the original multi-agent problem. Sufficient conditions for the main results were also derived.

The disturbance set over-approximation we use to obtain γ may, in some cases, be a very gross approximation. Its consequences to our approach's performance are one of the problems that remains to be solved in the future. A more important open problem is that of extending our solution to the multi-agent network in a distributed fashion, without having just one agent deciding on where should the formation go next.

Appendix A

Appendix

A.1 Disturbance Set Estimation

Derivation 1 (Extension of the empirical rule to the bivariate normal distribution) *Given the ellipsoid centered at μ and shape matrix M ,*

$$\mathcal{E}(\mu, M) = \{x \in \mathbb{R}^n : (x - \mu)^T M^{-1} (x - \mu) \leq 1\}$$

the probability of a N -dimensional random variable $X \sim N(\mu, \Sigma)$ lying inside it is

$$\begin{aligned} P[X \in \mathcal{E}(\mu, M)] &= \int_{\mathcal{E}(\mu, M)} f_x(x) dV_x \\ &= \int_{\mathcal{E}(\mu, M)} \frac{1}{(2\pi)^{\frac{N}{2}} \det(\Sigma)^{\frac{1}{2}}} e^{-\frac{1}{2}(x-\mu)^T \Sigma^{-1} (x-\mu)} dV_x \\ &= \frac{1}{(2\pi)^{\frac{N}{2}} \det(\Sigma)^{\frac{1}{2}}} \int_{\mathcal{E}(\mu, M)} e^{-\frac{1}{2}(x-\mu)^T \Sigma^{-1} (x-\mu)} dV_x \end{aligned}$$

where dV_x is the infinitesimal volume element in the x space. Since Σ is a symmetric positive definite matrix, we can perform its Cholesky decomposition to obtain $\Sigma = CC^T$. Replacing x by $y + \mu$ (with the new infinitesimal volume element, dV_y being equal to dV_x), $\mathcal{E}(\mu, M)$ becomes $\mathcal{E}(0, M)$ and we now have

$$P[X \in \mathcal{E}(\mu, M)] = \frac{1}{(2\pi)^{\frac{N}{2}} \det(\Sigma)^{\frac{1}{2}}} \int_{\mathcal{E}(\mu, M)} e^{-\frac{1}{2}y^T (CC^T)^{-1} y} dV_y$$

Note that

$$\begin{aligned} y^T (CC^T)^{-1} y &= y^T (C^T)^{-1} C^{-1} y \\ &= y^T (C^{-1})^T C^{-1} y \\ &= (C^{-1} y)^T C^{-1} y \end{aligned}$$

Performing the following change of variable

$$\begin{aligned} z &= C^{-1} y \\ dV_z &= \det(C^{-1}) dV_y \end{aligned}$$

where dV_z is the infinitesimal volume element in the z -space, the ellipsoid $\mathcal{E}(0, M)$ becomes

$$\begin{aligned} \mathcal{E}(0, M) &= \{z \in \mathbb{R}^n : y^T M^{-1} y \leq 1\} \\ &= \{z \in \mathbb{R}^n : (Cy)^T M^{-1} (Cz) \leq 1\} \\ &= \{z \in \mathbb{R}^n : z^T C^T M^{-1} Cz \leq 1\} \end{aligned}$$

and since we are interested in the particular case where $M = k\Sigma = kCC^T$,

$$\begin{aligned} \mathcal{E}(0, k\Sigma) &= \{z \in \mathbb{R}^n : z^T C^T (kCC^T)^{-1} Cz \leq 1\} \\ &= \{z \in \mathbb{R}^n : k^{-1} z^T C^T (C^T)^{-1} C^{-1} Cz \leq 1\} \\ &= \{z \in \mathbb{R}^n : z^T C^T (C^T)^{-1} C^{-1} Cz \leq k\} \\ &= \{z \in \mathbb{R}^n : z^T z \leq k\} \\ &= \mathcal{B}_{\sqrt{k}}(0) \end{aligned}$$

The probability of the sample lying in the ellipsoid is now

$$P[X \in \mathcal{E}(\mu, M)] = \frac{1}{(2\pi)^{\frac{N}{2}} \det(\Sigma)^{\frac{1}{2}}} \int_{\mathcal{B}_{\sqrt{k}}(0)} e^{-\frac{1}{2} z^T z} \det(C) dV_z$$

and since

$$\begin{aligned} \det(\Sigma)^{\frac{1}{2}} &= \det(CC^T)^{\frac{1}{2}} \\ &= (\det(C) \det(C^T))^{\frac{1}{2}} \\ &= (\det(C)^2)^{\frac{1}{2}} \\ &= \det(C) \end{aligned}$$

we have

$$P[X \in \mathcal{E}(\mu, M)] = \frac{1}{(2\pi)^{\frac{N}{2}}} \int_{\mathcal{B}_{\sqrt{k}}(0)} e^{-\frac{1}{2} z^T z} dV_z$$

We are interested in $N = 2$ (bivariate normal distribution). For two dimensions, $\mathcal{B}_{\sqrt{k}}(0)$ can be easily parametrized using polar coordinates,

$$z = [r \cos(\theta), r \sin(\theta)]^T$$

$$dV_z = r dr d\theta$$

and

$$\begin{aligned} P[X \in \mathcal{E}(\mu, M)] &= \frac{1}{2\pi} \int_{\mathcal{B}_{\sqrt{k}}(0)} e^{-\frac{1}{2}z^T z} dV_z \\ &= \frac{1}{2\pi} \int_0^{2\pi} \int_0^{\sqrt{k}} e^{-\frac{1}{2}r^2} r dr d\theta \\ &= \frac{1}{2\pi} \int_0^{2\pi} d\theta \int_0^{\sqrt{k}} e^{-\frac{1}{2}r^2} r dr \\ &= \int_0^{\sqrt{k}} e^{-\frac{1}{2}r^2} r dr \\ &= - \left[e^{-\frac{1}{2}r^2} \right]_0^{\sqrt{k}} \\ &= 1 - e^{-\frac{k}{2}} \\ &= 1 - \frac{1}{\sqrt{e^k}} \end{aligned}$$

This yields the following results

k	$P[X \in \mathcal{E}(\mu, k\Sigma)]$
1	0.3945
2^2	0.8647
3^2	0.9889
4^2	0.9997

Bibliography

- [1] K.J. Astrom and B.M. Bernhardsson. Comparison of riemann and lebesgue sampling for first order stochastic systems. In *Decision and Control, 2002, Proceedings of the 41st IEEE Conference on*, volume 2, pages 2011–2016 vol.2, Dec. 2002.
- [2] João Borges de Sousa, Karl Henrik Johansson, Jorge Silva, and Alberto Speranzon. A verified hierarchical control architecture for coordinated multi-vehicle operations. *International Journal of Adaptive Control and Signal Processing*, 21(2–3):159–188, 2007. Special issue on autonomous adaptive control of vehicles.
- [3] Giorgio Buttazzo and Luca Abeni. Adaptive workload management through elastic scheduling. *Real-Time Syst.*, 23(1/2):7–24, 2002.
- [4] A. Cervin and J. Eker. Feedback scheduling of control tasks. In *Decision and Control, 2000. Proceedings of the 39th IEEE Conference on*, volume 5, pages 4871–4876 vol.5, 2000.
- [5] Chandra, Ramesh and Liu, Xue and Sha, Lui. On the Scheduling of Flexible and Reliable Real-Time Control Systems. *Real-Time Syst.*, 24(2):153–169, 2003.
- [6] João Borges de Sousa. Notes on concepts and interpretation of control systems. Available at <http://paginas.fe.up.pt/~jtasso/notes.pdf>, April 2008.
- [7] J. P. Desai, J. Ostrowski, and V. Kumar. Controlling formations of multiple mobile robots. *Proc. of IEEE Int. Conf. on Robotics and Automation*, pages 2864–2869, 1998.
- [8] Reinhard Diestel. *Graph Theory*. Springer-Verlag, electronic edition, 2005.
- [9] Dimos Dimarogonas and Karl H. Johansson. Event-triggered cooperative control. In *European Control Conference, 2009. Proceedings of the*, pages 3015–3020, August 2009.
- [10] Dimos V. Dimarogonas and Kostas J. Kyriakopoulos. A connection between formation infeasibility and velocity alignment in kinematic multi-agent systems. *Automatica*, 44(10):2648–2654, 2008.
- [11] M. Haque and M. Egerstedt. Decentralized formation selection mechanisms inspired by foraging bottlenose dolphins. *Mathematical Theory of Networks and Systems*, 2008.
- [12] A. J. Healey. ME4823 Dynamics of Marine Vehicles. Naval Postgraduate School, Monterey, California, 2009.
- [13] E.G. Hernandez-Martinez and E. Aranda-Bricaire. Non-collision conditions in multi-agent robots formation using local potential functions. In *Robotics and Automation, 2008. ICRA 2008. IEEE International Conference on*, pages 3776–3781, May 2008.

- [14] G. Lafferriere, A. Williams, J. Caughman, and J.J.P. Veerman. Decentralized control of vehicle formations. *Systems and Control Letters*, 54(9):899–910, 2005.
- [15] Z. Lin, B. Francis, and M. Maggiore. Necessary and sufficient graphical conditions for formation control of unicycles. *IEEE Transactions on Automatic Control*, 50(1):121–127, 2005.
- [16] C. L. Liu and James W. Layland. Scheduling algorithms for multiprogramming in a hard-real-time environment. *J. ACM*, 20(1):46–61, 1973.
- [17] S. Mastellone, D.M. Stipanovic, C.R. Graunke, K.A. Intlekofer, and M.W. Spong. Formation control and collision avoidance for multi-agent non-holonomic systems: Theory and experiments. *International Journal of Robotics Research*, 27(1):107–126, 2008.
- [18] J A Mattias Green and Anders Stigebrandt. Statistical models and distributions of current velocities with application to the prediction of extreme events. *Estuarine, Coastal and Shelf Science*, 58(3):601–609, 2003.
- [19] D. Seto, J.P. Lehoczky, L. Sha, and K.G. Shin. On task schedulability in real-time control systems. In *Real-Time Systems Symposium, 1996., 17th IEEE*, pages 13–21, Dec 1996.
- [20] Jorge Silva and João Borges de Sousa. Models for simulation and control of underwater vehicles. In Harald Aschemann, editor, *New Approaches in Automation and Robotics*, chapter 11, pages 197–206. I-Tech Education and Publishing, Vienna, Austria, May 2008.
- [21] P. Tabuada. Event-triggered real-time scheduling of stabilizing control tasks. *Automatic Control, IEEE Transactions on*, 52(9):1680–1685, Sept. 2007.
- [22] Xiaofeng Wang and M.D. Lemmon. Event-triggered broadcasting across distributed networked control systems. In *American Control Conference, 2008*, pages 3139–3144, June 2008.
- [23] F. Xie and R. Fierro. On motion coordination of multiple vehicles with nonholonomic constraints. *American Control Conference*, pages 1888–1893, 2007.